Progress in Gamma Detection for Basic Nuclear Science and Applications

J. Simpson, Science and Technology Facilities Council, Daresbury Laboratory and A. J. Boston, University of Liverpool

https://doi.org/10.1093/acrefore/9780190871994.013.93
Published online: 30 January 2024

Summary

The atomic nucleus, consisting of protons and neutrons, is a unique strongly interacting quantum mechanical system that makes up 99.9% of all visible matter. From the inception of gamma-ray detectors to the early 21st century, advances in gamma detection have allowed researchers to broaden their understanding of the fundamental properties of all nuclei and their interactions. Key technical advances have enabled the development of state-of-the art instruments that are expected to address a wide range of nuclear science at the extremes of the nuclear landscape, excitation energy, spin, stability, and mass. The realisation of efficient gamma detection systems has impact in many applications such as medical imaging environmental radiation monitoring, and security. Even though the technical advances made so far are remarkable, further improvements are continually being implemented or planned.

Keywords: gamma detection, nuclear science, nuclear application, germanium semiconductor detectors, high-resolution γ spectroscopy, tracking technology

Subjects: Measurement Science, Instrumentation, Metrology, Nuclear Physics, Particles and Fields

1. Introduction

The atomic nucleus, consisting of protons and neutrons, is a unique strongly interacting quantum mechanical system that makes up 99.9% of all visible matter. The goal of nuclear science is to realize a detailed understanding of the fundamental properties of all nuclei and their interactions. Indeed, nuclear physics research seeks to answer some fundamental questions about the universe, such as what governs the structure and behavior of atomic nuclei, what are the limits of nuclear existence, and how many nuclei are there. Many of these questions can be answered by studying excited states in nuclei using the technique of γ-ray spectroscopy. Indeed, the study of the γ-decay properties of nuclei has provided an enormous quantity of information on the behavior of nuclei when they are stressed, for example, by the application of high temperatures, high angular momentum, large values of isospin (proton/neutron ratio), or large deformation. Properties that can be measured by γ spectroscopy include the excitation energy, spin and parity of states, nuclear moments, and lifetimes. These properties, when compared with early 21st-century theoretical nuclear models, give a more informed understanding of nuclear matter.

This article focuses on germanium semiconductor detectors that are the best choice for high-resolution γ spectroscopy. Advances in the use of Ge detectors are reviewed from their inception to the early 21st century. Gamma spectroscopy started with the development of NaI(Tl) scintillation detectors in the 1950s. It then evolved to use Ge(Li) detectors in the 1960s and high-purity Ge detectors in the 1970s, driven by the requirement of having better energy resolution. Large arrays of Ge detectors were then assembled, but it was the development of the first arrays of escape suppressed spectrometers (ESSs) that had arguably the most impact on modern spectroscopy. An ESS comprises a Ge detector surrounded by a scintillation detector to reject events caused by Compton scattered γ rays that do not deposit all their energy in the Ge, resulting in vastly improved spectral response. ESS arrays have evolved over the last 3 decades, and many still operate today.

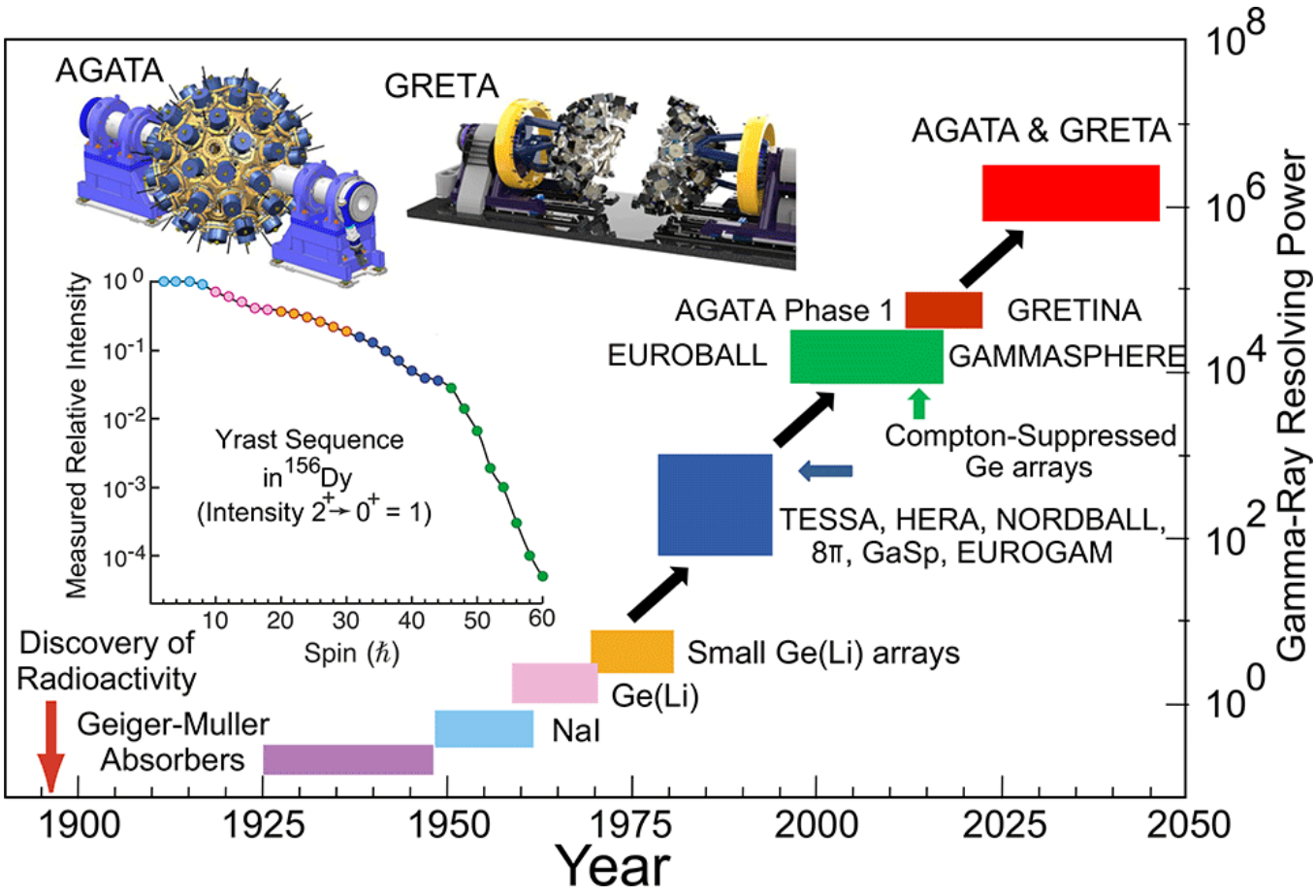

Figure 1. Evolution of gamma-ray detection technology through the decades (Wyss & Riley, 2022). The gamma-ray resolving power is a measure of the ability to observe the faint emissions from rare and exotic nuclear states and is directly related to the observable intensity within a nucleus. The insert shows the intensity of the yrast (lowest energy for a given spin) transitions in a typical nucleus (^{156}Dy) as a function of spin. The Advanced GAmma Tracking Array and Gamma Ray Energy Tracking Array tracking arrays will have a significant increase in resolving power.

The present major advance in γ-ray spectroscopy is the realization of the tracking of a γ ray as it scatters and deposits its full energy in the detector volume. Tracking involves the use of highly segmented Ge crystals and pulse shape analysis to determine the energy, time, and position of every interaction. The resulting system will have vastly improved efficiency and spectral response.

This technical advance is driven by the need to identify ever weaker transitions in nuclei far from the line of stability, in the heaviest nuclei, in highly excited states, and at the highest angular momentum. It coincides with the new generation of radioactive ion beam facilities that are coming online and the continuing development of stable beam facilities. Two major tracking spectrometers, the Advanced GAmma Tracking Array (AGATA) in Europe and the Gamma Ray Energy Tracking Array (GRETA) in the United States will both utilize this new tracking technique and are moving toward their full implementation.

In addition to basic nuclear science, γ-ray spectroscopy is used in neutrino physics and in many applications, such as medical imaging, environmental monitoring, nuclear waste assay, nuclear decommissioning, and security systems. These are wide-ranging, and a few examples in which the imaging techniques associated with the realization of tracking are discussed.

2. Detector Developments Over the Years

2.1 Development of High-Resolution Gamma Detection Systems

2.1.1 From NaI(Tl) to Ge(Li) and High-Purity Ge Detectors

Early attempts to measure the properties of excited states in the atomic nucleus via γ-ray spectroscopy were made with a few sodium iodide, NaI(Tl), scintillation detectors that were developed in the late 1940s. NaI(Tl) has rather poor energy resolution Full Width Half Maximum (FWHM $\sim$ 90 keV at 1,300 keV) and at that time had a low efficiency, which limited the sensitivity of these experiments. Nevertheless, early experiments were able to establish the low-spin ($I \leq 8 - 10\hbar$) rotational structure of nuclei (Morinaga & Gugelot, 1963), identifying transitions of intensity $\approx$ 2% that of the lowest $2^+ \rightarrow 0^+$ decay, the strongest decay in an even–even nucleus. Large arrays of scintillation detectors were subsequently developed for nuclear spectroscopy. They consisted of shells of NaI(Tl) detectors arranged around a target. Examples include the 72-element spin spectrometer at Oak Ridge National Laboratory, United States (Jääskeläinen et al., 1983) and the 162-element Crystal Ball at Heidelberg, Germany (Simon, 1980). Although such arrays were efficient energy calorimeters and capable of detecting most of the energy emitted in the γ-ray cascade following a reaction, their application to discrete line γ-ray spectroscopy was limited by the relatively poor energy resolution of NaI(Tl).

A major step forward came with the development of reverse-biased semiconductor Ge detectors in the mid-1960s. The first Ge detectors had very small active volumes, limited by the high impurity concentration in the crystal. This was solved by drifting lithium into the crystal to

compensate for the naturally occurring p-type impurities in Ge (Freck & Wakefield, 1962; Pell, 1960; Tavendale & Ewan, 1963), to produce the Ge(Li) detector. The big advantage over NaI(Tl) is that Ge has very good energy resolution, typically ≤ 1 keV at 122 keV to ≈ 2 keV at 1,332 keV. This enables excited states in the complex-level schemes of nuclei to be resolved, resulting in a myriad of nuclear structure phenomena to be observed and studied. Ge(Li) detectors and the availability of numerous accelerator facilities had a tremendous impact on nuclear spectroscopy from the 1960s to ≈ 1980. Indeed, using just two Ge(Li) detectors, the phenomenon of nuclear backbending was first observed at the Research Institute for Physics, Stockholm, Sweden (Johnson et al., 1971, see also Wyss & Riley, 2022). This observation stimulated the field of both experimental and theoretical nuclear structure physics. It wasn't long before excited states were observed up to spin $I \sim 20 - 30\hbar$ in several bands in the same nucleus, an example being in ^{160} Yb (Riedinger et al., 1980), with the use of just four Ge(Li) detectors. Further developments of Ge(Li) detectors took place including, for example, the segmentation of the outer contact (Simpson et al., 1983) and detectors with more than one crystal in the same cryostat, for example (Eube et al., 1975). Segmentation and multiple crystals are now commonplace in modern spectroscopy.

The next development, in the late 1970s, was the production of high-purity Ge (HPGe) crystals (Hall & Soltys, 1971; Hansen, 1971) based on a closed-end coaxial geometry. Crystals of low impurity concentration for both p-type and n-type could be grown such that with a reasonable bias of ≈5,000 V, a large volume detector could be manufactured. HPGe detectors have several advantages over Ge(Li), including that they can be stored at room temperature; are quicker to produce, avoiding the long Li drift times in manufacturing; and can be n-type as well as p-type. The latter is important for in-beam nuclear physics experiments since n-type HPGe detectors suffer much less from neutron-induced radiation damage than p-type (or Ge(Li)'s). These advantages resulted in commercial production of Ge(Li) ending around 1980.

In order to track the improvement in the power of detector spectrometers, the lowest intensity that can be resolved in a nuclear decay is a key indicator. Figure 1 shows the γ-ray resolving power as a function of time for key technical advancements and spectrometer array developments. The resolving power is defined as the inverse of the γ-ray intensity compared with the intensity of the lowest energy $2^+ \rightarrow 0^+$ transition. This schematic figure shows, for example, that prior to the use of ESS arrays (see the section "ESS Arrays"), it was possible to observe transitions at the level of several percent. This enabled, in a few cases, the observation of states up to a spin of $36 - 38\hbar$ (e.g., the lowest energy collective rotational band in ^{158} Er; Burde et al., 1982) and the intrinsic aligned states in ^{152} Dy (Khoo et al., 1978).

2.1.2 ESS Arrays

A huge step forward in nuclear gamma spectroscopy came with the use of arrays of ESSs. Ge or Ge(Li) detectors have excellent energy resolution; however, they have an experimental problem in that they have very poor signal-to-noise ratios in their energy spectra. Using a bare detector and a standard ^{60} Co source (which has two γ rays at 1,173 and 1,332 keV) produces a spectrum in which only ~ 20% of the counts are in the full-energy photopeaks. The remaining ~ 80% of the counts form a continuous background at lower energies caused mainly by γ rays Compton

scattering out of the Ge crystal. The solution is to detect this scattered radiation in a surrounding detector (an ESS) and reject coincident events between the Ge detector and the suppression shield. The combination is termed an ESS. This technique, suggested by Ewan and Tavendale (1964), was developed with a combined Ge(Li) detector with a NaI(Tl) ESS in experiments at Chalk River in Canada in the late 1960s (Alexander et al., 1968) and in the Netherlands (Beetz et al., 1977). The first array of escape-suppressed Ge detectors for in-beam experiments was built in 1980 in Riso, Denmark by a collaboration of the Niels Bohr Institute and the Universities of Liverpool and Manchester in the United Kingdom. The array, called TESSA (The Escape Suppressed Spectrometer Array), consisted of five Ge(Li) detectors and NaI(Tl) ESSs (Sharpey-Schafer & Simpson, 1988; Twin, 1985).

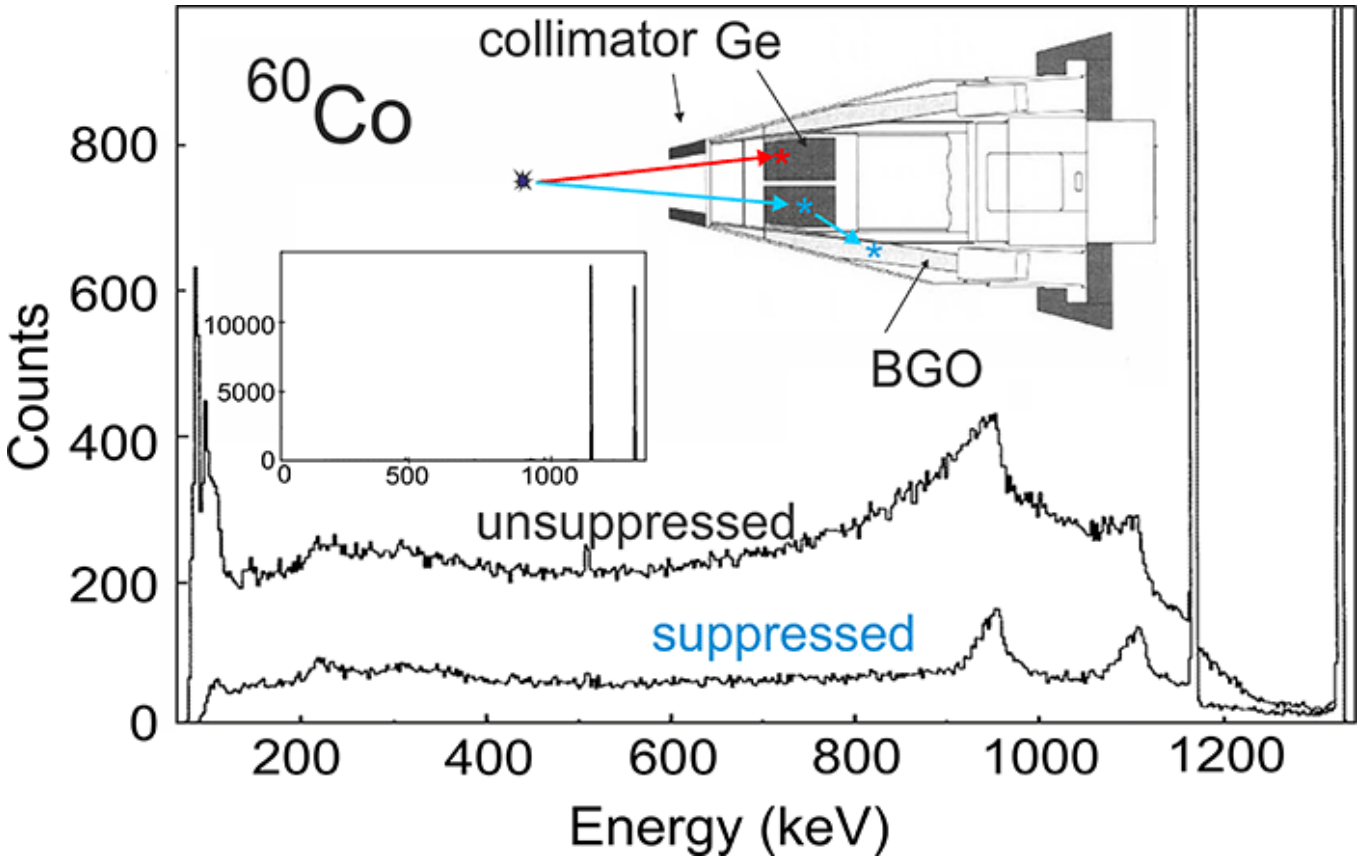

Figure 2. Unsuppressed and suppressed spectra from a ^{60}Co source. The main *y*-axis scale is expanded to show the background below the photopeaks. The spectrum is from a typical escape suppressed spectrometer.

The spectra obtained with ESSs have an excellent peak-to-total ratio (P/T) of ≈60%. A typical suppressed and unsuppressed Ge spectrum from a ^{60}Co source is shown in Figure 2, where the reduction in the background below the photopeaks in ^{60}Co is clearly demonstrated. This improvement in the P/T is crucial in coincidence spectroscopy. For example, in a doubles ($\gamma - \gamma$ or γ^2) coincidence experiment, the photopeak–photopeak coincidence probability is proportional to $(\mathrm{P/T})^2$. Therefore, for ^{60}Co, using a suppression shield typically results in an

improvement of more than a factor of 8 in the photopeak coincidences when compared with the background. Even larger improvements are obtained when higher fold-coincidence events are recorded.

This first TESSA spectrometer had a considerable impact on the development of further arrays. However, the physical size of NaI(Tl) shields limited the number of ESSs that could be placed around a target to 5–6. A significant step was the use of much more compact suppression shields to enable more ESSs to be used, hence increasing the efficiency. The High Energy Resolution Array (HERA) at the Lawrence Berkeley Laboratory (United States; Diamond, 1985) was the first to combine bismuth germanate (BGO) suppression shields with n-type HPGe detectors. BGO has a higher average Z and density than NaI(Tl) resulting in a three times more efficient system per interaction length. HERA comprised 21 ESSs, with a total photopeak efficiency at 1.3 MeV of 15%, enabling sufficient triple $(\gamma - \gamma - \gamma)$ coincidences to be collected in a few days of beam time.

By the mid-1980s, many arrays worldwide with 20 ESSs having total peak efficiencies of 0.5% -1.0% were constructed, for example, TESSA3, United Kingdom (Nolan et al., 1985; Twin et al., 1983); Chateau de Cristal, France (Beck, 1984); Osiris, Germany (Lieder et al., 1984); Nordball (Herskind, 1986); 8π spectrometer, Canada (Martin et al., 1987); and HERA. One of these arrays, TESSA3, was used in the discovery of the classic discrete line superdeformed (SD) band in ^{152} Dy (Twin et al., 1986) in the mid-1980s. Such SD structures carry about 1%–2% of the individual nucleus production cross section. Arrays with this level of sensitivity enabled a plethora of nuclear structure phenomena to be discovered and investigated. These arrays were mostly funded by individual nations (except Nordball, which was a Scandinavian collaboration). The first major multinational collaboration was the ESSA30 set up at Daresbury Laboratory, United Kingdom, in the mid-1980s, which combined ESS systems from Germany, Italy, Scandinavia, and the United Kingdom. Such collaborations became important in the next stages of array development, particularly in Europe.

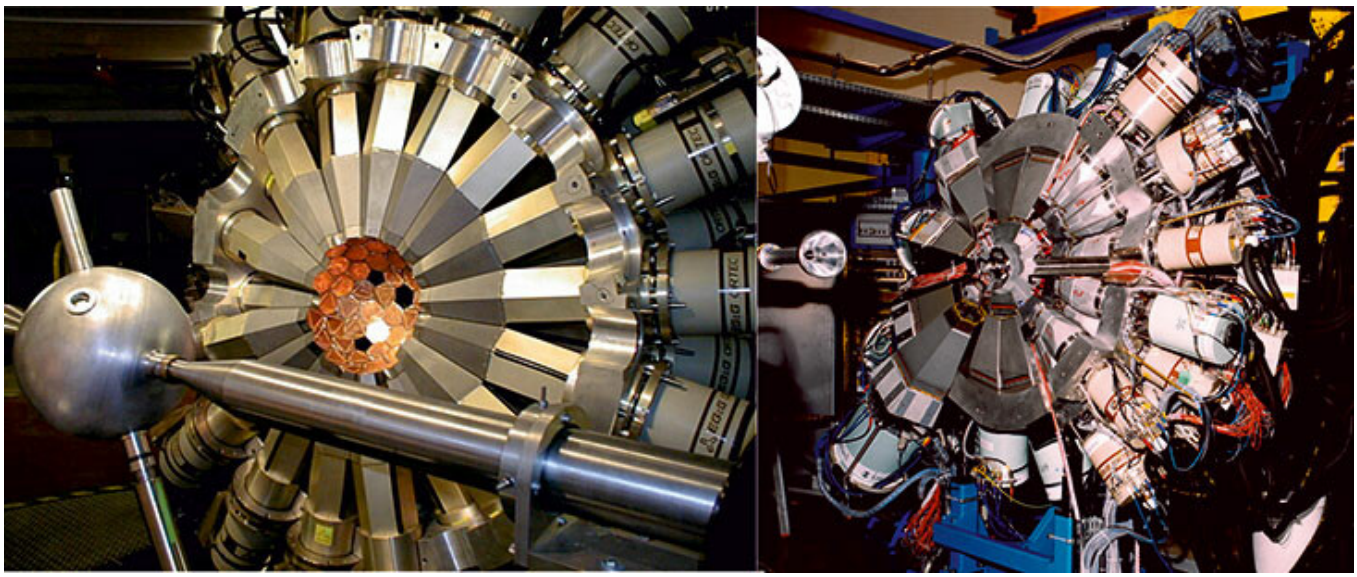

Figure 3. The Gammasphere (left) and EUROBALL IV (right) spectrometers.

The drive for more efficiency and better sensitivity led to the realization of even bigger and better arrays in the 1990s. These included the spectrometers GaSp, Eurogam, and EUROBALL in Europe and Gammasphere in the United States. They incorporated some key technical advances including the use of detectors with electrical segmentation of the outer contacts, the use of multiple crystals in the same cryostat, and crystal encapsulation.

GaSp and Eurogam I started operation at Legnaro National Laboratory (LNL), Italy, and Daresbury Laboratory, United Kingdom, respectively, in 1992. GaSp (Alvarez, 1993) comprised 40 ESSs, each with a single-crystal Ge detector surrounded by a BGO suppression shield, and had a total photopeak efficiency of 6% in a compact geometry. Eurogam I (Beausang et al., 1992), a U.K.–France collaboration, had 45 ESSs, again with single Ge detectors and BGO shields.

These arrays with single crystal Ge detectors had some limitations in performance. One issue was the Doppler broadening of the γ-ray line shape, caused by the recoiling nuclei moving at a high velocity following a reaction, which is most apparent at 90° to the beam direction. There was a need for a higher granularity of the detectors to reduce the solid angle subtended. In the Eurogam project, the Clover detector was developed (Duchêne et al., 1999), which consists of four Ge crystals closely packed in the same cryostat. The individual crystals were slightly smaller than those in the single-crystal ESSs, which give better spectral performance (resolution) especially around 90° and a high efficiency when the scattering between the crystals is included in an event. Clover detectors are included in many arrays worldwide. They were first deployed in Eurogam II at CRN-Strasbourg, France in 1994. Eurogam II had two rings of 12 clover detectors, each in a suppression shield, around 90°, with 15 ESSs, with single-element Ge detectors in both the forward and backward directions. The total photopeak efficiency of Eurogam II was $\approx$8%.

In parallel with the Clover development was the production of an even larger composite detector comprising seven n-type HPGe detectors, called the Cluster detector (Eberth et al., 1990). The technique of encapsulation of the crystals was developed by a collaboration between the University of Köln, KFA Julich, Germany, and the company Eurysis Mesures (Eberth et al., 1996). Encapsulation involves decoupling the crystal vacuum from the cryostat vacuum by mounting the Ge crystal in a sealed aluminum can (capsule), in principle for its entire life, thus avoiding any surface contamination. Another advantage of encapsulation is that the capsule can be handled directly and annealed (following in-beam neutron damage) in an oven. The cluster has a very high efficiency even for high energy, up to 10 MeV. Arrays of up to six Cluster detectors were used at several facilities in the mid-1990s.

In the mid-1990s, a European collaboration involving France, Germany, Italy, Scandinavia, and the United Kingdom decided to pool its detectors to build a 4π spectrometer called EUROBALL (Simpson, 1997). EUROBALL III consisted of 30 single-crystal ESSs from Eurogam and GaSp in the forward direction, 26 suppressed Clover detectors in two rings around 90°, and 15 suppressed Cluster detectors in the backward direction. This array with 239 Ge detectors had a total photopeak efficiency of 10%, which is close to the maximum that can be achieved with an array of ESSs. It operated for 2 years from 1997 at LNL, Italy, and was then moved to the Vivitron accelerator at IReS Strasbourg, France, from 1999 to 2003, where an inner ball of 210 BGO detectors was added for reaction channel selection. This array was called EUROBALL IV.

In the late 1980s, a proposal was developed in the United States to build a 4π spectrometer, Gammasphere, based on a single type of ESS. The device comprised up to 110 ESSs of single-crystal Ge detectors with BGO suppression shields (Lee, 1990) and had a total photopeak efficiency of ≈10%. The overall performance of Gammasphere was improved with the implementation of segmentation of the outer boron implanted contact into two halves (Lee et al., 2003) in order that the contact with the first hit could be identified. An overall improvement of resolution from 5.5 to 3.9 keV was achieved in-beam for a recoil velocity of v/c = 0.02.

Gammasphere and EUROBALL IV (see Figure 3) had similar efficiency and resolving power enabling, in some cases, transitions at a level below 10^{-4} of the $2^+ \rightarrow 0^+$ to be observed (see Figure 1).

2.1.3 Arrays for Radioactive Beam Facilities

In the early 21st century, nuclear structure physics is moving toward the study of the most exotic nuclei close to and beyond the drip lines. This is the scientific motivation for the new radioactive ion-beam facilities. In reactions with these, often low-intensity beams, very exotic nuclei are produced at very low reaction cross sections, sometimes at high-recoil velocities, and decay among high-radiation backgrounds. Gamma spectrometers with very high efficiency and resolution are mandatory, hence the requirement for composite and segmented detectors.

Exogam (Azaiez, 1999; Simpson et al., 2000) was constructed for experiments at SPIRAL, GANIL. This array comprises up to 16 segmented Clover detectors with BGO suppression shields. Each crystal in the Clover is longitudinally segmented into four segments (Shepherd et al., 1999). The TIGRESS spectrometer (Scraggs et al., 2005) at TRIUMF in Canada has a similar design to Exogam, but the Clovers have an additional transverse segmentation, effectively resulting is a Clover with 32 segments. The SeGa array operated at the National Superconducting Cyclotron Laboratory at Michigan State University (MSU). This array had 18 highly segmented Ge detectors segmented into four longitudinally and eight ways in the transverse directions. By arranging the crystals such that the transverse segments faced the beam direction, then the overall solid angle for each segment was small; therefore, the energy resolution is optimized.

The Miniball array (Eberth, 1997; Eberth et al., 2001; Habs, 1997) took developments to the next level in determining the position of interaction. This array, designed for use at REX-ISOLDE and CERN, utilized highly segmented and encapsulated Ge crystals and was the first to use digital electronics to record the preamplifier pulse shapes. The encapsulated detectors in Miniball were segmented six ways longitudinally on its outer contact to provide a first level of position-of-interaction information. The signal from the core of the detectors records the full energy of the signal. In addition, by recording the pulse shape, the radial position of interaction can be measured from the rise time of the net charge signal. As the charge carriers (electrons and holes) flow to the contacts, transient charges are induced in the neighboring segments. By measuring the amplitude of these induced charges, the azimuthal position of interaction can also be determined. This position determination effectively increases the granularity of each detector

from 6 to 100 and, with a 40-detector setup, to 4,000, which is significantly greater than 170 and 240 for Gammasphere and EUROBALL, respectively. An extra transverse segmentation was included on the later Miniball detectors to increase this granularity even further.

3. The Development of the 4π Tracking Spectrometers

3.1 The Principle of Tracking

The desire for significantly higher efficiency and greater sensitivity driven by the science interest requires the realization of a 4π Ge shell. ESS arrays are limited by the total solid angle that can be subtended by the Ge since up to ≈50% is occupied by the collimators mounted on the suppression shield; see the insert in Figure 2. Removing the suppression shields could, in principle, enable the total photopeak efficiency to be significantly increased. However, without position sensitivity in the detectors, it is not possible to distinguish two or more interactions in the same detector or one γ ray interacting and scattering in two or more detectors. The feasibility of a Ge shell requires more than 1,000 detectors to be able to isolate each interaction in a high-multiplicity event.

The solution is the concept of γ-ray tracking, first proposed by the Berkeley group (Deleplanque et al., 1999; Lee et al., 2003). The requirement is to identify all interactions as the original photon scatters in the array and order them in time. This cannot be achieved directly because the detector has insufficient time resolution to order the interactions. Instead, algorithms are used to reconstruct the interactions with the knowledge of the energy, time, and, importantly, the position of each interaction. The tracking array concept is shown schematically in Figure 4.

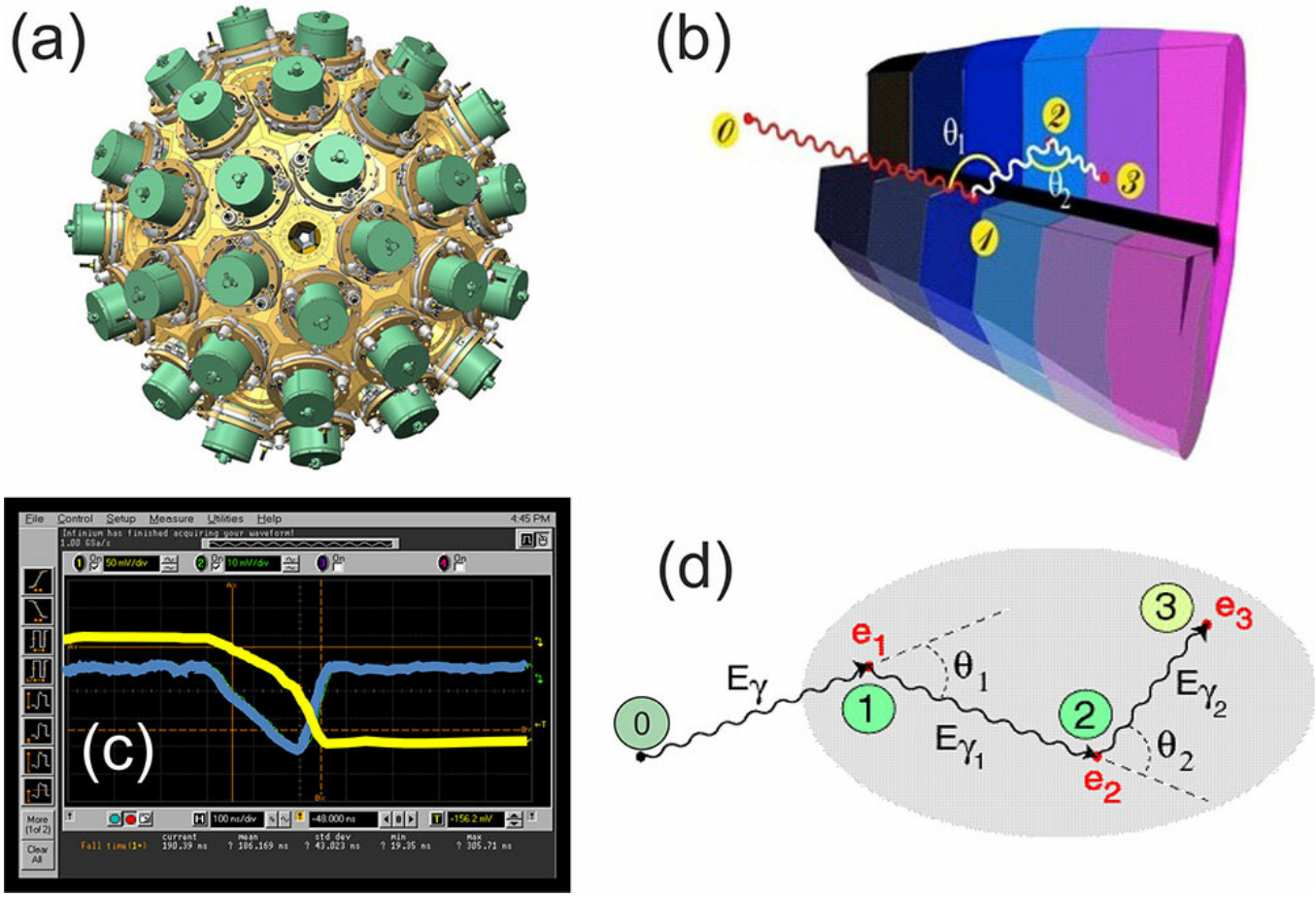

Figure 4. The ingredients of gamma-ray tracking. (a) CAD design of the 4π array. (b) Highly segmented HPGe crystal. (c) Pulse shapes that are used to determine position, energy, and time using pulse shape analysis. (d) Reconstruction of the full event in software using tracking algorithms.

In order for a tracking array to be realized, a system with a position resolution of a few millimeters and an energy resolution of 2–3 keV for every interaction is required (Kröll & Bazzacco, 2001; Lopez-Martens et al., 2004; Schmid et al., 1999; Vetter et al., 2000). For a typical coaxial Ge crystal 2.7 in. (7 cm) in diameter and 3.5 in. (9 cm) in length, this would require a detector that comprises 30,000 individual detector elements or voxels. This is not feasible by segmentation alone, hence the requirement of pulse shape analysis (PSA) and digital electronics. Several projects tested the feasibility of producing such tracking detectors. These included the MARS project (Kröll & Bazzacco, 2001), which employed 24-fold segmented tapered coaxial detectors; in the United Kingdom, 24- and 36-fold segmented detectors were developed (Descovich et al., 2005; Valiente-Dobón et al., 2003); and the Berkeley group investigated a 36-fold segmented detector (Vetter et al., 2000). These projects demonstrated, by scanning the detectors with collimated γ rays, that the required position resolution could be achieved. Very highly segmented planar Ge detectors, with segmentation on both contacts, were also investigated. They have sufficient segmentation to avoid the need for PSA. However, dead regions around the active volume (guard rings, support, etc.) resulted in the conclusion that for a 4π system, coaxial detectors were the best option.

3.2 Technical Developments for a 4π Tracking Spectrometer

The technical developments being made, and the scientific motivation, were the key ingredients to realize 4π tracking spectrometers. Two major tracking spectrometers (Lee & Simpson, 2010), AGATA (Akkoyun et al., 2012) in Europe and GRETA (Lee et al., 2003) in the United States, are implementing this tracking technology. The GRETINA (Gamma-Ray Energy In-Beam Nuclear Array) project is the first phase of the GRETA project, covering 1/4 of 4π (Lee et al., 2004; Paschalis et al., 2013). This review focuses on the AGATA spectrometer; however, many of the technological ingredients and solutions are essentially the same for GRETINA/GRETA.

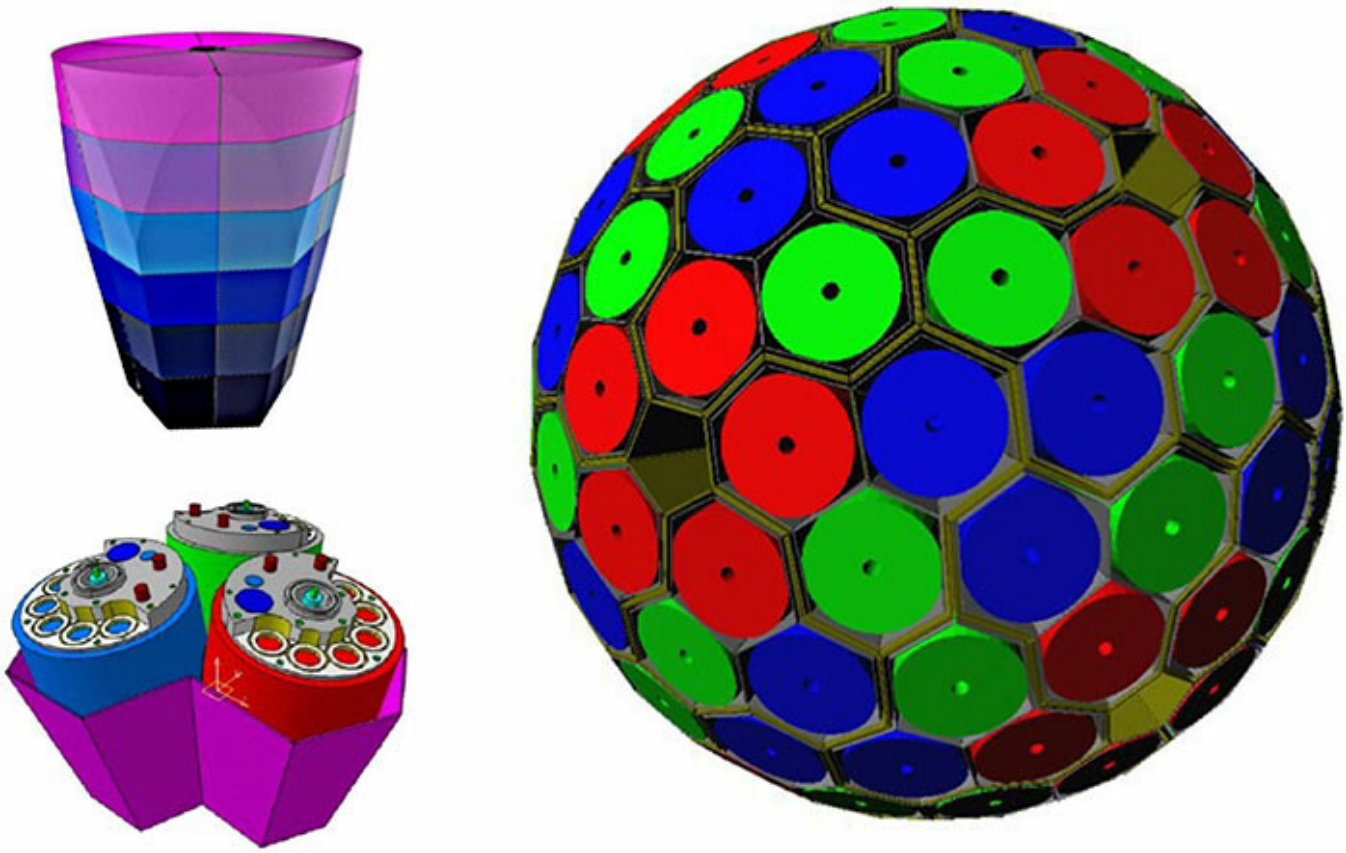

Figure 5. CAD image of one segmented Ge crystal, the three slightly different encapsulated tapered hexagonal crystals and the 180 geometry for Advanced GAmma Tracking Array.

There are many technical components needed for a tracking spectrometer. The crucial ones are the highly segmented Ge detectors; the digital electronics to record the pulse shapes; PSA algorithms to identify the position, energy, and time of each interaction; and the tracking algorithms to reconstruct the full interaction of a γ ray. These are described in later sections. A review of the many aspects of software needed to operate the AGATA spectrometer is given by Stézowski et al. (2023). The complex mechanical structure and the many infrastructure components needed for detector operation for AGATA (including the liquid nitrogen filling system, high- and low-voltage systems, myriad of cabling, earthing requirements, and a database of all components) are reviewed by Smith et al. (2023).

The detectors in AGATA and GRETA are 36-fold segmented, encapsulated Ge detectors. Figure 5 shows a Computer Aided Design (CAD) image of the segmented Ge crystal. To optimally cover a 4π geometry, the design for AGATA is based on a structure with 180 tapered hexagons and 12 pentagons. This design was optimized using GEANT4 calculations to maximize the efficiency (Farnea et al., 2010). The final design is of three slightly different shapes for the tapered hexagonal crystals, all ≈3.1 in. (8 cm) in diameter at the rear, with a 10° angle, and ≈3.5 in. (9 cm) long. These are grouped in threes and mounted in a cryostat, with the same design for all capsules, that provides the liquid nitrogen cooling and houses the preamplifiers and associated signal and temperature monitoring cables. The 12 pentagons in the geometry are used for beam in/out and services, including cables and support. A photograph of the triple cryostat with, for illustration, a transparent end cap, is shown in Figure 6a, and Figure 6b shows 11 triple cryostats (39 detectors) mounted in LNL in 2022. The GRETA geometry is based on a similar design with 120 hexagons with two different crystal shapes in groups of four capsules per cryostat.

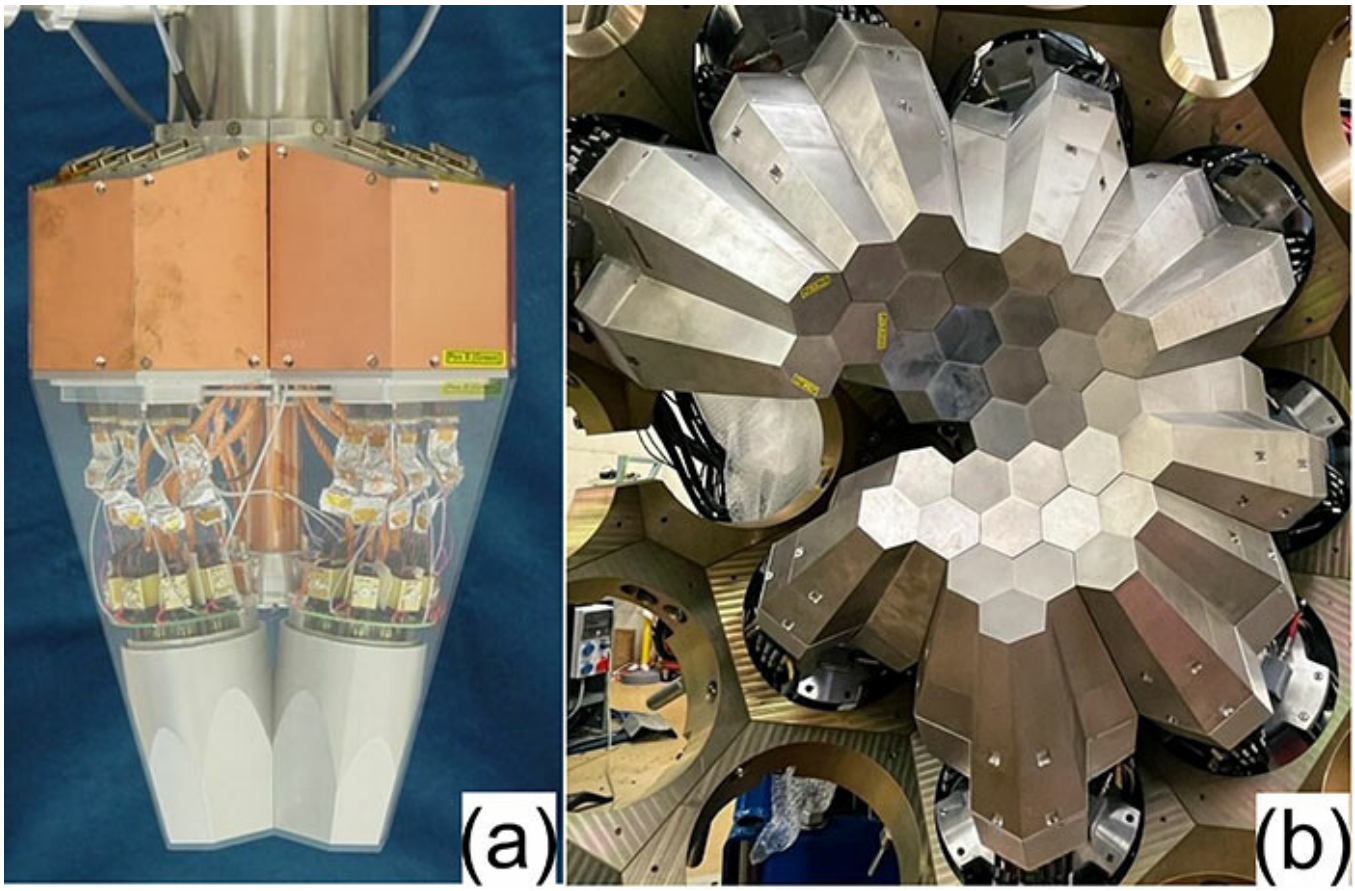

Figure 6. (a) Photograph of an Advanced GAmma Tracking Array triple cluster with a “transparent” endcap to show the Ge detector capsules and front-end electronics within the cryostat. (b) Photograph of 11 AGATA Triple Clusters (ATCs) mounted in the array at Legnaro National Laboratory in 2022.

3.2.1 Digital Electronics

Modern electronics systems now use digital, rather than analogue, electronics. Digital electronics offers a number of major advantages over conventional analogue-based systems, such as improved stability, increased count rate capability, improved noise performance, time-stamped list mode data acquisition, and, importantly, enabling PSA. In a digital electronics system, the preamplifier signal from the detector is directly digitized (typically at 100 MHz sampling frequency and 14-bit dynamic range), and all subsequent signal processing is handled in a software environment. This removes the requirement for multiple different analogue processing units, greatly reducing the complexity of the required signal-processing electronics per channel. A major advantage of this approach is that the digital system is much more stable over time. If there are environmental changes, such as humidity or temperature changes, analogue systems are prone to variations in the signal amplitude through the processing chain, which manifest as drifts in the position of the observed photopeak. These gain drifts need to be tracked over time, and temperature stabilization of systems was often required. In a digital system, particularly one using a cryogenic semiconductor detector such as HPGe, these drifts are eliminated.

Digital systems offer a hugely increased count rate capability, due to the fact that digital electronics utilize fast algorithms to extract the time and energy of the incident γ ray. The energy is typically extracted utilizing a trapezoidal filter, the software equivalent of the analogue gated integrator, as part of a moving window devolution algorithm. These algorithms allow the precise extraction of the deposited energy from the signal waveform with little to no dead time losses up to a count rate of 80–100 kHz when implemented in a field programmable gate array, which is integrated into the digital electronics. In a typical analogue system, using Gaussian shaping, the count rate limitation is a few tens of kHz.

Digital electronics continuously record the signal waveform, which allows for further software processing of the detector signal, facilitating PSA, where the unique characteristics of the waveform shape can be used to infer information on the location of the γ-ray interaction. This information has always been part of the signal waveform, but analogue systems have been unable to utilize this information.

A bespoke digital electronics system is required to record and process the 37 signal waveforms from the AGATA and GRETINA/GRETA detectors. The specification of the AGATA electronics is to operate at a count rate of 50 kHz per crystal, using 100-MHz 14-bit ADC sampling for the 36 segments, and provide two energy ranges for the core signal (to 7 and 20 MeV), with a 100 MHz clock distribution providing 10-ns time-stamping. The electronics pass the digital information for 1 μs for each signal to the AGATA computer farm for PSA and tracking. This challenging specification required an increase in the functionality of the electronics and the data acquisition system, which necessitated a custom-built system (Collado et al., 2023).

3.2.2 Detector Characterization and PSA

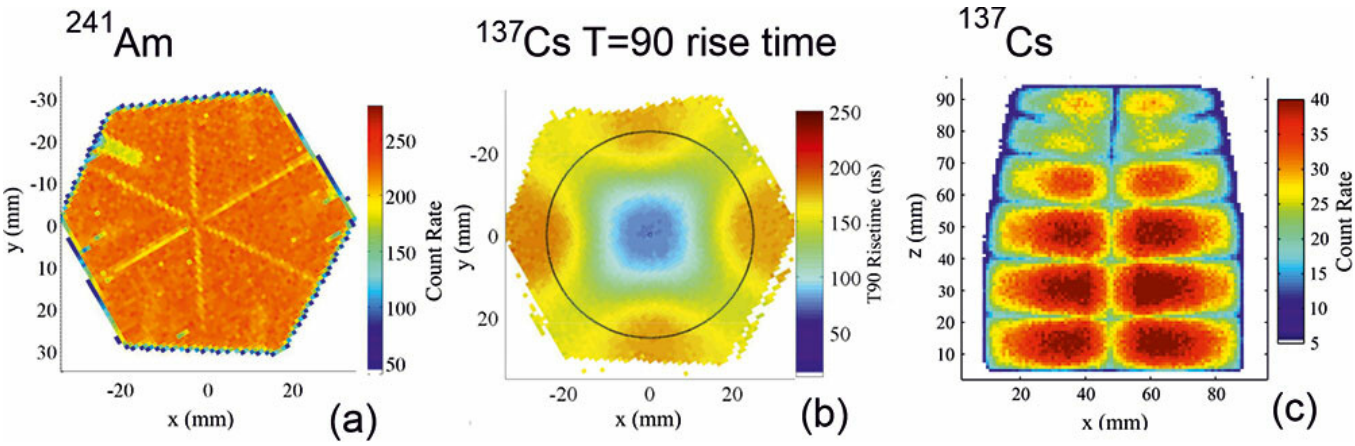

Figure 7. Example plots from two-dimensional scans of an Advanced GAmma Tracking Array capsule (see Colosimo et al., 2015). (a) Intensity plot from $^{241}\mathrm{Am}$ (60 keV) source scan with the detector in the vertical orientation showing surface effects. (b) T90 rise time plot from $^{137}\mathrm{Cs}$ source scan (662 keV). T(90) is the time for the signal to reach 90% of its full value. (c) $^{137}\mathrm{Cs}$ scan with the detector in the horizontal orientation showing interactions throughout the detector bulk.

PSA is an essential step in the recovery of the true interaction position of incident γ rays. The output of the PSA provides the input to the subsequent γ tracking algorithms that probabilistically combine the information returned by the PSA to reconstruct the individual γ tracks. The aim of PSA is to determine the number of interactions in a segment or crystal and reconstruct their individual positions, times, and the deposited energies by analyzing the experimental preamplifier signals. The real-time processing requirement of the AGATA data acquisition system and the requirements of the tracking algorithms impose stringent performance requirements on the PSA algorithms. To perform a Doppler correction and achieve the best possible (P/T), the interaction locations have to be resolved with a precision of on average 0.19685 in. (5 mm; FWHM). For PSA to be used in experiments with high beam intensities, the reconstruction should take ≈1 millisecond per event. In AGATA, PSA is performed at the per crystal or local level, while γ ray tracking is performed at the array or global level. The AGATA collaboration has investigated the performance of a number of different approaches to achieving the optimum PSA performance.

To determine the position of interaction from PSA, a knowledge of the signal shapes and amplitudes as a function of position and energy in the crystals is required. This is either from a full calculation of the signals as a function of position or measuring the pulse shapes experimentally by scanning the crystals with a radioactive source to fully characterize the properties of the crystal. Comparison is then made between the measured pulse shapes in all segments for each interaction with either the calculated or experimental database of signals.

In AGATA and GRETA, several scanning systems have been developed to provide experimental pulse shapes throughout the detector volume. They use a collimated γ-ray source, producing a pencil beam of γ rays to select interactions at a particular position inside the detector volume.

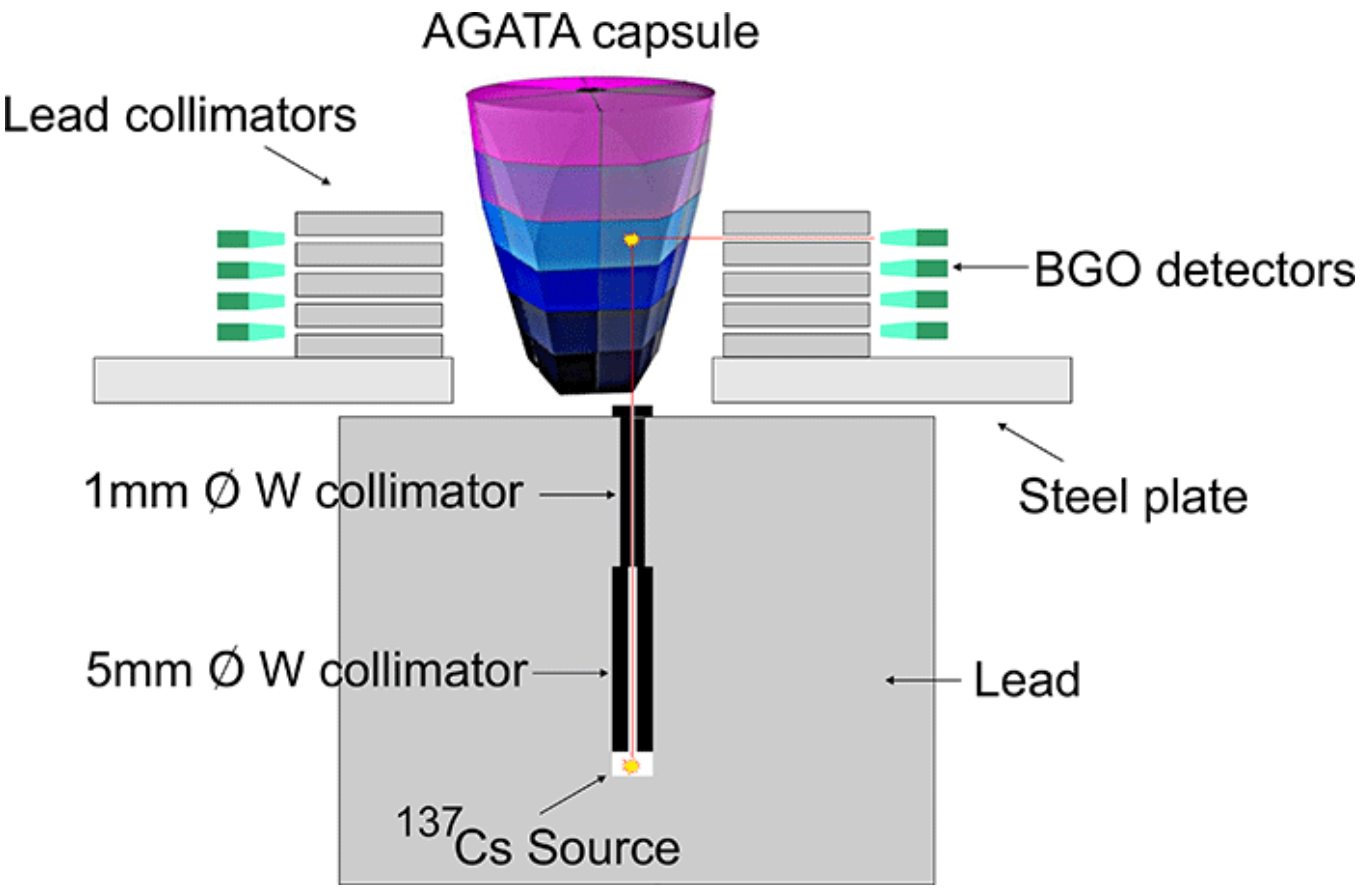

Figure 8. Schematic diagram of the University of Liverpool coincidence scanning system. A ^{137}Cs source is positioned along the *X*- and *Y*-axes by the scanning table. γ rays emitted from the source, that scatter ≈90° inside the detector, pass through the secondary lead collimators and are stopped in an array of 40 bismuth germanate scintillation detectors. The secondary collimation constrains the interaction position along the *z*-axis.

The simplest scanning technique, often used as a first stage of a full characterization is "singles" scanning. Here, the γ-ray interaction position is only known in two dimensions, so a fully constrained study of the detector cannot be made, but geometrical information, as well as surface and bulk performance, can be studied by appropriately choosing the γ-ray energy used.

The collimated source is mounted on an automated two-axis (*X*, *Y*) positional table, which allows the position of the source to be precisely controlled. The detector being characterized is then mounted above the table, in either the vertical or horizontal orientation, such that the beam of γ rays impinges on an active area of the detector. The *XY* position of interaction within the detector is inferred from the position of the scanning table. The source is raster scanned across the detector in a uniform grid, typically of 0.0019–0.0787 in. (0.5–2.0 mm) steps, and a database

of detector response as a function of interaction position is recorded. Basic characterization information can be obtained such as the count rate (intensity) and charge collection time (rise time) plots, as shown in Figure 7.

A technique developed at the University of Liverpool (Nelson et al., 2007) for localizing the depth of interaction in the z-axis is referred to as "coincidence" scanning. This is an extension of the "singles" scanning but allows γ-ray interaction positions to be constrained in three dimensions through the use of secondary collimation and ancillary detectors. The detector being characterized is surrounded by a series of lead collimators, with 0.0787–0.1811-in. (2–3-mm) spaces between them, which are aligned with specific depths in the detector undergoing characterization, as shown in Figure 8. These secondary collimators allow γ rays to escape if they scatter within the detector at 90° with respect to the primary collimation. Each secondary collimator is surrounded by a number of BGO scintillation detectors to detect these scattered γ rays. A 662-keV γ ray undergoing a single 90° Compton scatter will deposit 374 keV in the AGATA crystal and the remaining 288 keV in the scintillator. Selecting appropriate energies in the offline data analysis on both detectors allows only true single-site interactions to be selected and processed.

The benefits of this technique are that it gives a very precise knowledge of the three-dimensional (3D) position of interaction (2 mm^3) within the detector. In addition, the time of the interaction within the AGATA detector can be deduced from the fast and predictable response of the BGO detectors. This provides a more precise measure of the start of the charge collection (t_0) than what is possible using the AGATA detector alone. Accurate identification of t_0 is crucial for comparing experimental and simulated pulse shapes. The disadvantages are that the secondary collimation results in a very low efficiency, so measurement times can be very long (many hours per position), leading to partial scans taking several months to complete to ensure sufficient statistics are recorded. This means that it is not practical to scan the entire volume of a crystal. Therefore, a subset of positions must be chosen that represents the most interesting area of the crystal for comparison with, and validation of, the more comprehensive simulated data sets.

Since experimental scanning of a full crystal is so time-consuming, a calculated database of pulse shapes is required. The AGATA Data Library (ADL) was developed for the calculation of signals. The ADL (Bruyneel et al., 2016) introduces the general concepts and basic assumptions required. Knowledge of the electrical field inside the detector relies on the solution to the Poisson equation for the complex AGATA detector geometry. The movement of the charge carriers is affected by many factors including the direction of travel with respect to the crystal axis orientation. This can result in a variation of the charge carrier drift time of up to 30% in the high field regime; therefore, 3D mobility models are employed both for electrons and holes in Ge, at near–liquid nitrogen temperature.

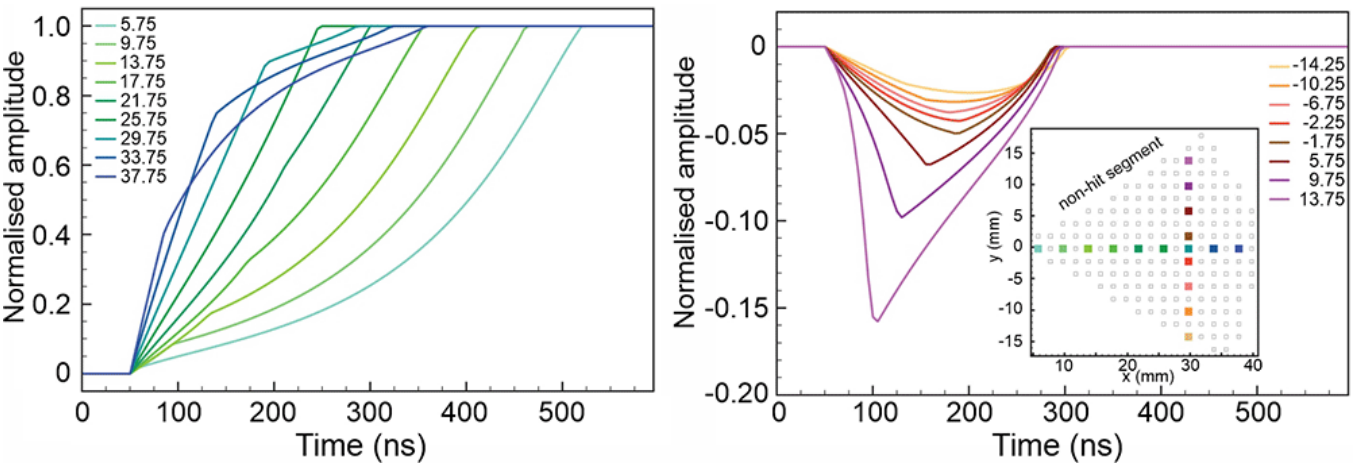

Figure 9. Calculated traces from the AGATA Data Library for an Advanced GAmma Tracking Array detector. In the left plot, the core signals for different interaction radii (mm) are shown. The different mobility of electrons and holes is visible as a discontinuity in the rising edge. For small radii, the faster electrons are collected immediately while the slower holes still have to drift to the segment electrode. The shortest rise time occurs at an intermediate position; for larger radii, the time of the electrons to be collected is longer than for the holes. The right plot shows the transient signals in a segment adjacent to the hit segment. The amplitude of the transient signal depends on the distance (mm) of the interaction to the non-hit segment. The slice is 1.5 in. (40.25 mm) from the front of the detector (Bruyneel et al., 2016).

Once the trajectories of all free charges in the detector are calculated as a function of time, the induced signals in each of the electrodes are determined. The weighting potential for each of the electrodes of interest is calculated for every position in the sensitive volume of the detector. The time evolution of the induced charge and the integral of the current into the electrode are given by the charge-weighted sum of the weighting potential evaluated at the position of the free charges.

In Figure 9, examples of calculated traces from ADL for an AGATA detector are shown where a realistic response function of the acquisition electronics is taken into account (Bruyneel et al., 2016). The response function of the preamplifier is also included, which is measured by the injection of a clean fast rectangular pulse in the preamplifier's pulser input. The cross-talk in segmented AGATA detectors was also studied, see Bruynell, Reiter, Wiens, Eberth, Hess, Pascovici, Warr, and Weisshaar (2009). For AGATA detectors, two types of cross-talk have been observed to contribute: (a) Proportional cross-talk creates a cross-talk signal in neighboring electrodes proportional to the capacities between the electrodes involved. Accurate routines were developed to measure and correct for this type of cross-talk within AGATA (Bruynell, Reiter, Weins, Eberth, Hess, Pascovici, Warr, Aydin, et al., 2009). (b) Differential cross-talk induces a signal that is proportional to the derivative of the induced signal and therefore dependent on the rise time of the inducing signal. Since the derivatives of active segment signals are only non-zero during the rise time of the inducing signal, this second type of cross-talk can have an impact on the performance of the PSA. A detailed discussion can be found in Bruynell, Reiter, Weins, Eberth, Hess, Pascovici, Warr, and Weisshaar (2009). The comparison between measured signals and calculated signals from a fine grid of points in the crystal is performed in both AGATA and

GRETINA using an adaptive grid search (AGS) method. This works by searching for one or two interaction points per segment. In the AGATA implementation, the algorithm searches were restricted to one interaction point in a segment. If experimentally multiple hits occur in a single segment, then this implementation considers the energetic barycenter of these positions as the location of the interaction. The interaction positions are determined by the optimization of a figure of merit that compares experimental signals against a basis of pre-computed responses. Due to the significant trace length and number of electrodes used in AGATA, individual signal comparisons are computationally intensive, and an exhaustive search does not meet the execution rates necessary for online PSA. Instead, a coarse grid approximation is applied using the AGS algorithm (Venturelli & Bazzacco, 2005) that determines the coarse optimum of the basis followed by a refined search, which finds the closest match to the experimental signal. Figure 10 shows a comparison between experimental pulses in all segments for an interaction in one segment, compared with the best fit from the calculation. The AGS algorithm produced a position resolution of ≈0.19685 in. (5 mm) with a performance of ≈2 kHz throughput (Recchia et al., 2009), which meets the requirements of the γ-ray tracking (Farnea et al., 2010).

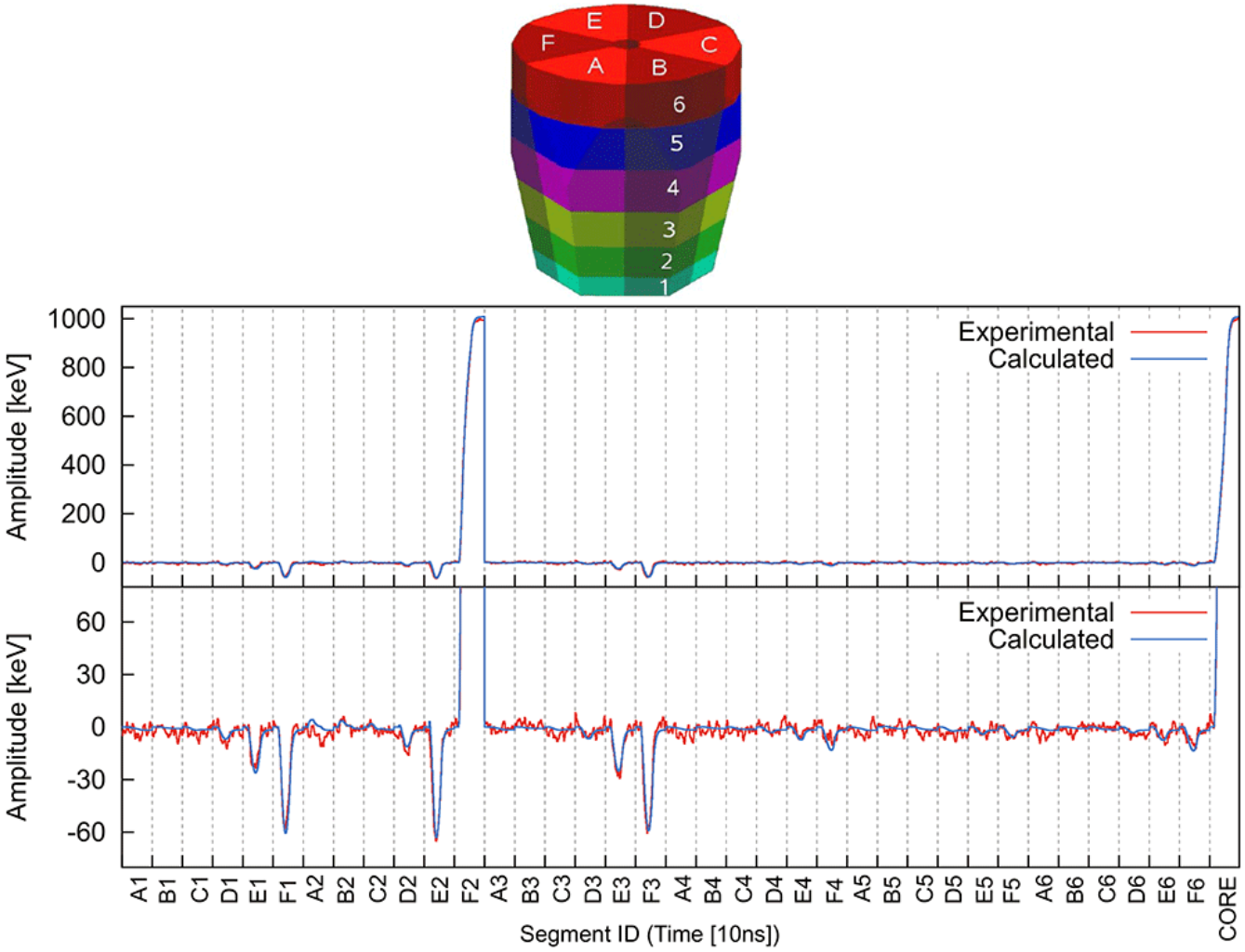

Figure 10. The best match determined by the grid search algorithm of a random interaction scaled to the right energy compared with experimental data. The horizontal axis is split in 37 sections, each containing a 600 ns trace of the corresponding electrode. The image shows the labeling scheme of the segments. The top plot is scaled to full energy deposition. The bottom plot is expanded to emphasize the transient signals. The main interaction is in segment F2. Transient signals are clearly seen in segments F1, F3, and E2. A reduced signal in A2 compared with E2 gives azimuthal position information of the interaction.

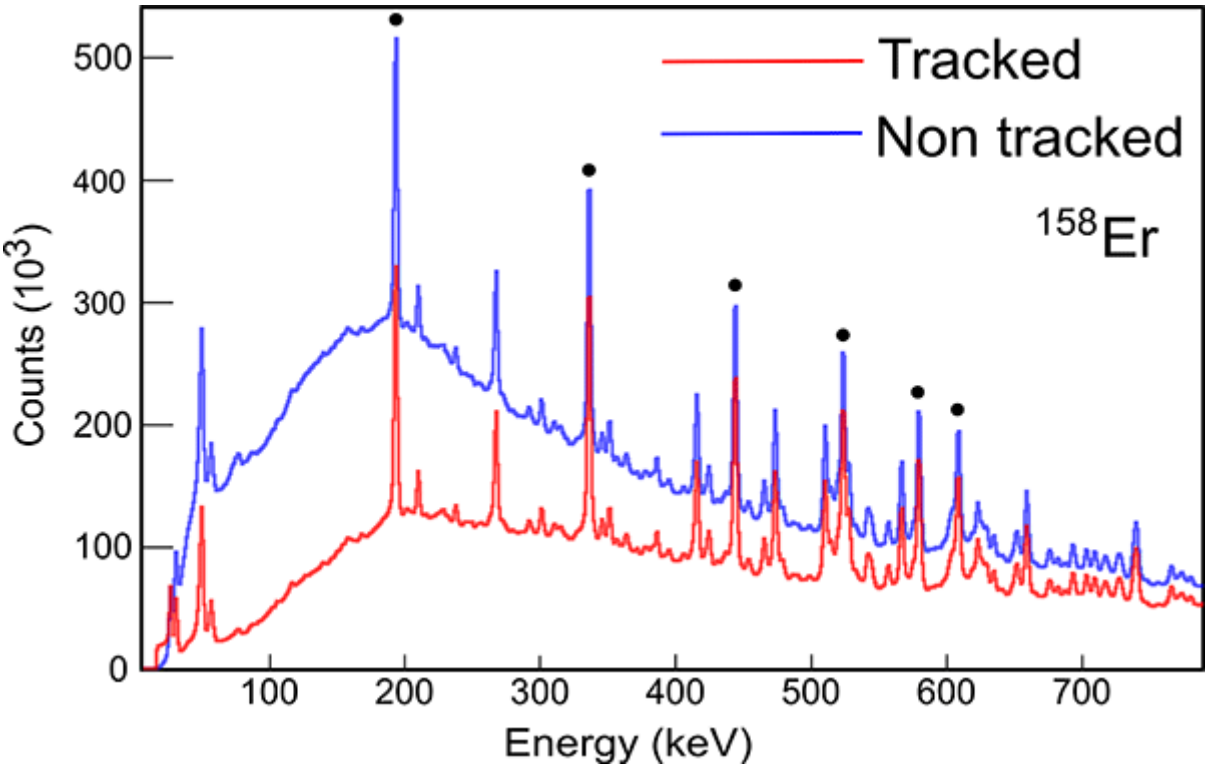

Figure 11. In-beam spectra following the reaction $^{122}\mathrm{Sn} + {}^{40}\mathrm{Ar}$ at 170 MeV in which the strongest reaction channel is $^{158}\mathrm{Er}$; the lowest six yrast transitions in $^{158}\mathrm{Er}$ are indicated by a filled circle. The spectra compare a non-tracked spectrum and a tracked spectrum from Advanced GAmma Tracking Array at GANIL with 22 detectors.

Source: Courtesy of A. Korichi.

3.2.3 Tracking

Once the position of interaction is determined by PSA, then with the energy of interaction, it is possible to reconstruct the γ-ray track as it fully deposits its energy. Tracking mainly involves the Compton scattering process since this is the dominant interaction process for γ rays in matter from about 150 keV up to several MeV. Gamma-ray tracking algorithms are based on the Compton scattering formula that involves the initial and final energy of the γ ray and the angle of scattering. There are two types of algorithms, so-called forward tracking and backward tracking. Forward-tracking algorithms start with the knowledge of the source of the radiation (the target in a reaction or source) and then track the interactions before final absorption. Backward-tracking algorithms start with the final photoelectric interaction point and reconstruct the track

back to the source. The AGATA and GRETINA/GRETA projects have developed tracking algorithms (Crespi et al., 2023; Korichi & Lauritsen, 2019). In both projects, forward-tracking algorithms are implemented because they provide a better performance.

The main algorithms developed for AGATA are the Mars Gamma Tracking algorithm (Bazzacco, 2004) and the Orsay Forward Tracking algorithm (Lopez-Martens et al., 2004). The GRETINA project has also implemented a forward-tracking algorithm (Lauritsen et al., 2016). These algorithms work by searching for clusters of interactions in three dimensions and determining possible groupings between interactions that satisfy the Compton scattering formula by varying the angle of scatter. The first implementations of tracking algorithms perform well, which has been demonstrated by with sources and in beam. Figure 11 compares non-tracked and tracked AGATA spectra, with 22 detectors, following the in-beam reaction $^{122}\mathrm{Sn} + {}^{40}\mathrm{Ar}$ at 170 MeV (Korichi & Lauritsen, 2019). The improvement using tracking in the peak to background is clearly demonstrated. However, they do have some limitations, and efforts are ongoing to improve the performance of both PSA and tracking.

3.3 The Status of the Tracking Arrays AGATA and GRETA and Future Plans

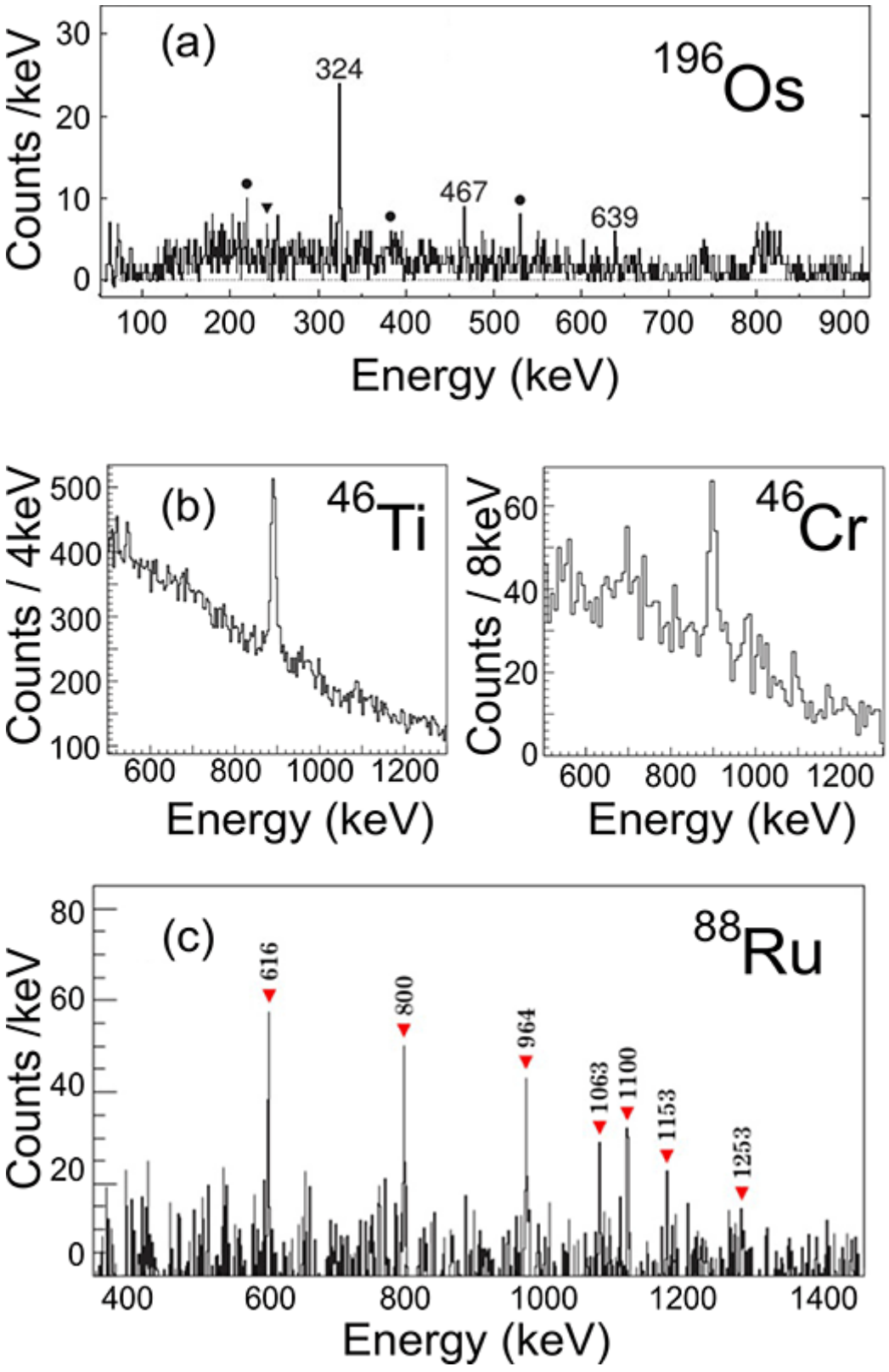

Figure 12. A highly selective set of spectra from Advanced GAmma Tracking Array. (a) The first three transitions in $^{196}\mathrm{Os}$ (John et al., 2014). (b) The $2^+ \rightarrow 0^+$ transitions in $^{46}\mathrm{Ti}$ and $^{46}\mathrm{Cr}$ obtained by relativistic Coulomb excitation (Boso et al., 2019). (c) The ground-state band in $^{88}\mathrm{Ru}$ (Cederwall et al., 2020).

The many technical developments to realize tracking, as discussed in Section 3.2, have demonstrated that the realization of a 4π spectrometer with photopeak efficiency of 40% at 1 MeV, as predicted in Farnea et al. (2010), will be achieved. AGATA and GRETA both had a research and development phase before starting science campaigns and improvements in many aspects are ongoing.

The GRETINA (Lee et al., 2004; Paschalis et al., 2013; Weisshaar et al., 2017) project is the first phase of GRETA and was commissioned in-beam in a series of engineering experiments in 2011 at the Lawrence Berkeley National Laboratory. Since then, it has operated in a series of science campaigns at the National Superconducting Cyclotron Laboratory at MSU and the Argonne National Laboratory. The project is evolving toward GRETA, where the final aim is the 4π array of 120 detectors. It will be a key research instrument at the new radioactive beam facility (Facility for Rare Isotope Beams) at MSU (Gade & Gelbke, 2010). The GRETA webpages include a detailed description of the project and a list of the wide range of publications (GRETA, 2023).

The AGATA project is an instrument that has operated and will continue to operate at major European facilities that deliver high-intensity, stable, and radioactive beams. It started in 2003 with a research and development phase to realize the ingredients needed to perform tracking. The first science campaign was at LNL, Italy from 2010 to 2011, with up to 15 detectors (Gadea et al., 2011). As the number of detectors increased gradually to 60, it subsequently operated at the GSI laboratory in Germany (Pietralla et al., 2014) from 2012 to 2014 and then at GANIL, France, from 2014 to 2021 (Clément et al., 2017). At each facility, it was coupled to a range of spectrometers, charged particle and neutron detectors, high-energy gamma detector arrays, fast-timing gamma systems, and instruments for specific measurements (e.g., for nuclear state lifetimes).

The project is now in its final phase to realize the 4π 180-detector array. This was motivated by the need for a more sensitive instrument to answer the scientific questions that will be addressed with the new radioactive beam and high-intensity stable beam facilities. Indeed, the 2017 NuPECC Long Range Plan for European nuclear physics (Bracco, 2017) supported the completion of the full geometry. The first deployment in this phase started in 2022 with a science campaign at LNL.

Each facility provides a wide range of beams and a variety of instrumentation and spectrometers that have enabled a rich and varied science program to be carried out (Bracco et al., 2021). Examples of some of the spectra obtained in this early phase of AGATA are shown in Figure 12. These are a tiny subset of spectra from a wide range of publications, all of which can be found in the AGATA project webpage (Nyberg, 2023). Figure 12a shows a spectrum of the first observation of transitions in the extremely neutron rich nucleus $^{196}\mathrm{Os}$ (John et al., 2014). This was obtained with just 15 detectors in AGATA's first science campaign at LNL and is part of an investigation of nuclear shape evolution across an isotopic chain. Figure 12b shows the spectra of lighter neutron-deficient nuclei, $^{46}\mathrm{Ti}$ and $^{46}\mathrm{Cr}$, that straddle the N=Z line (Boso et al., 2019). These spectra were obtained, with AGATA having 22 detectors, using the quite novel technique of relativistic Coulomb excitation of the selected nuclei that are moving at velocities of $\approx 50\%$ of the speed of light. This work is part of an investigation of charge symmetry and charge independence of the nuclear force. Figure 12c is a spectrum of the N=Z nucleus $^{88}\mathrm{Ru}$ obtained with 33 detectors at

GANIL (Cederwall et al., 2020) and displays evidence for isoscalar neutron–proton pairing correlations. These spectra demonstrate the wide range of physics that has already been investigated, with AGATA having only a fraction of 4π.

A detailed science case for AGATA was published in 2020 (Korten et al., 2020) to support its completion to 4π. This science case covers the nuclear landscape to the extremes of isospin toward and, beyond the drip lines, to the highest spins close to the fission limit and to the heaviest nuclei. The evolution of shell structure and magic numbers, the interplay between single-particle and collective degrees of freedom, shape coexistence, exotic shapes, and nuclear pairing are key topics of interest. Figure 13 shows some examples of the science that AGATA will address.

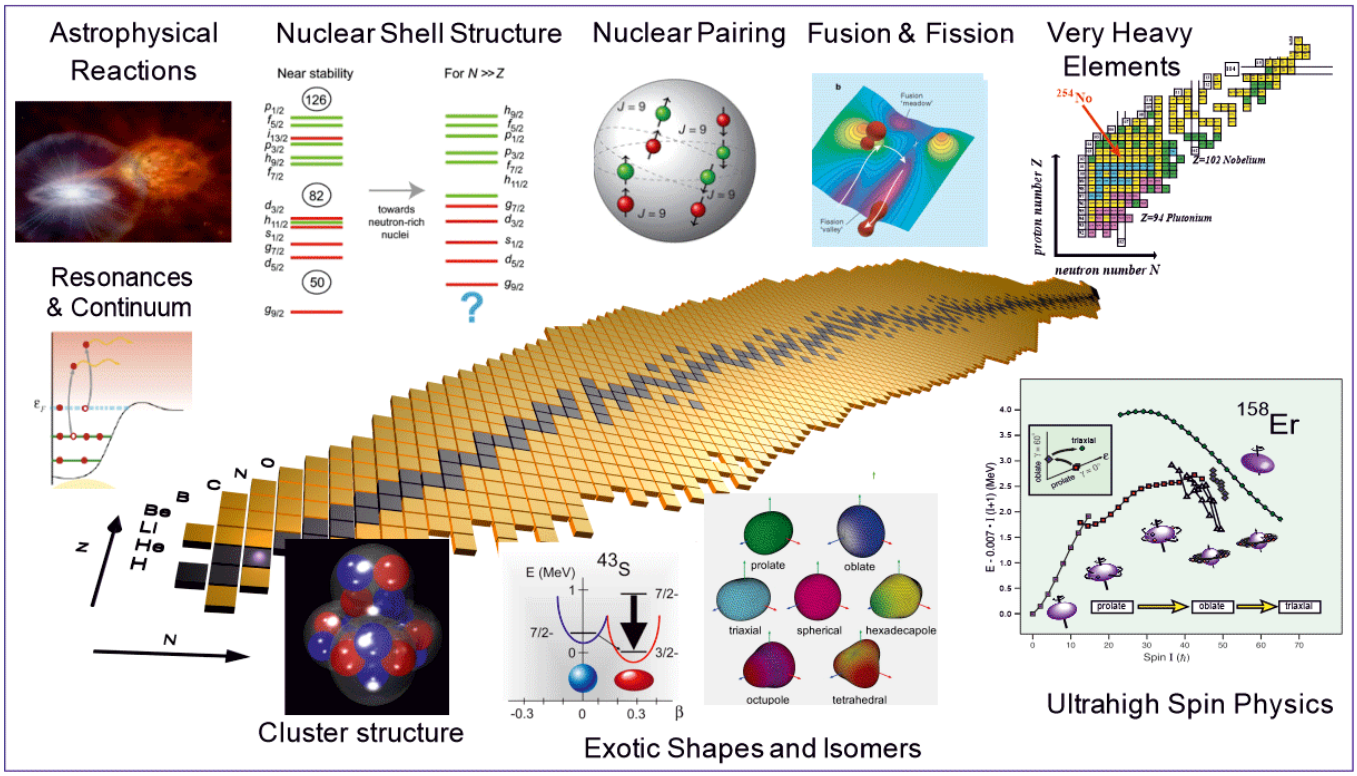

Figure 13. Illustration of some of the science that spans the nuclear landscape that can be addressed through γ-ray spectroscopy.

GEANT4 (Agostinelli et al., 2003; Allison et al., 2016) simulations have been performed to evaluate the performance of AGATA in its future implementations. A review of all aspects of simulations for AGATA can be found in Labiche et al. (2023). Two examples from the science case (Korten et al., 2020) are shown in Figure 14. The study of the very heaviest nuclei is of topical interest. The region around ^{254} No has been studied extensively, and this is providing excellent data on the orbitals close to the Fermi surface, giving insight into the location of the superheavy island of stability. The heaviest nucleus studied to date is ^{256} Rf; AGATA could enable even heavier nuclei such as ^{260} Sg to be studied by in-beam spectroscopy. Figure 14a shows the predicted improvement in the spectrum for ^{254} No from JUROGAM II (Eberth & Simpson, 2008) at Jyväskylä

Finland (a slightly modified version of Eurogam II) compared with a 3π AGATA (135 detectors). The study of nuclei at the limits of angular momentum and temperature is also at the forefront of nuclear structure science. A comparison of the lowest energy triaxial strongly deformed band in ^{158}Er (Paul et al., 2007; Simpson et al., 2023) calculated for EUROBALL compared with AGATA in its 4π (180 detectors) configuration is displayed in Figure 14b. The improvement in the signal-to-noise ratio for the highest energy/lowest intensity transitions is evident in this figure and is consistent with the predicted improvement in sensitivity of AGATA compared with previous spectrometers of up to two orders of magnitude (Korten et al., 2020; see Figure 1). This opens up spectroscopy at spins close to the fission limit and very high temperatures of, for example, hyper-deformed nuclei and Jacobi-shape transitions.

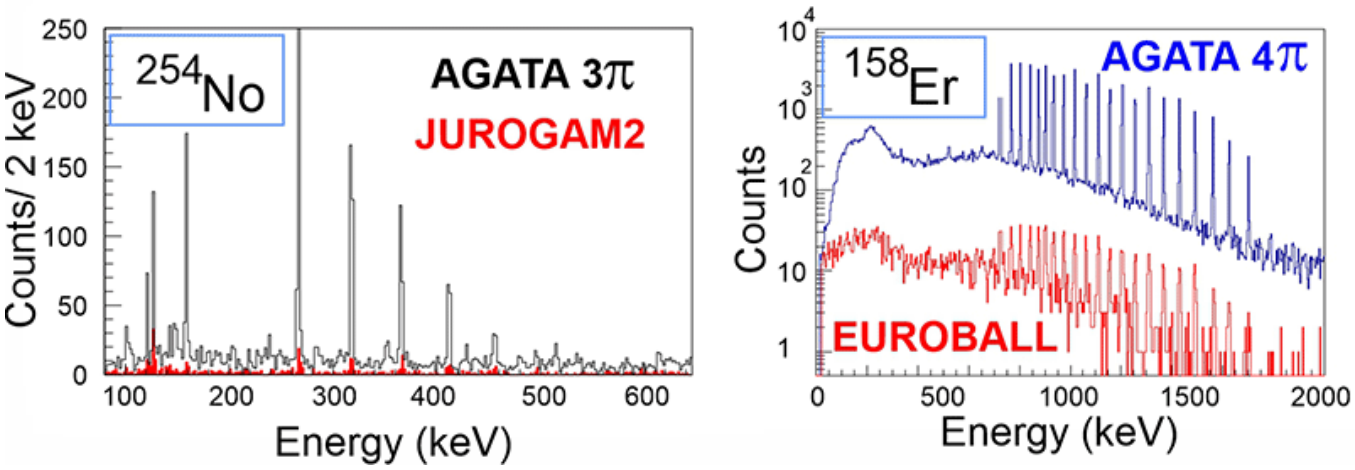

Figure 14. Specific examples of Advanced GAmma Tracking Array (AGATA) science. (Left) Spectroscopy of heavy nuclei. Comparison of calculated spectrum of ^{254}No using the existing JUROGAM II spectrometer at Jyväskylä compared with that for a 3π AGATA (135 detectors). (Right) High-spin studies. A comparison of the calculated spectrum of the lowest energy triaxial strongly deformed band in ^{158}Er using EUROBALL compared with that with a 4π AGATA (180 detectors).

4. Applications

Since the discovery of the atomic nucleus at the beginning of the 20th century, nuclear and particle physics research has driven the development of technologies that have had a huge societal impact. The development of the next-generation detector technologies, which utilize digital signal processing, has offered the potential for a step change in the performance of γ-ray-sensitive radiation detectors. One particular area of focus has been γ-ray imaging in areas such as medical imaging, environmental monitoring, security, and nuclear decommissioning. There are many examples of such imaging detector systems, and this article can only mention a few. Many of the technical developments for imaging systems, including digital systems and PSA and tracking, are similar to those required for the tracking spectrometers AGATA and GRETINA/GRETA.

In a parallel development by detector manufacturers, low-vibration mechanical cooling solutions have been developed. This enables the Ge detectors to be used without the requirement for liquid nitrogen.

4.1 Imaging Systems

With the exception of medical applications, γ-ray imagers usually require the capability to identify the location and activity of the radiation source in question, along with an accurate determination the particular isotope of origin. These requirements drive the design of commercially available systems, which utilize established technology to deliver a capability that is limited in performance by the design choices required. A good example of this is found in the nuclear decommissioning sector where an important part of the process is to demonstrate that the facility can return to a greenfield site. This is fulfilled through the reduction to a safe level of all radioactive contaminants present in the environment. During this, an emphasis is placed on in situ characterization and understanding of the environment that is to be made safe. A decommissioning environment presents a particular challenge due to the many radioisotopes that may be present.

Existing systems such as the RadScan:800 and RadScan:900 (Cavendish Nuclear, 2019) provide position-sensitive imaging through mechanical collimation of the incident gamma radiation but only achieve low- or medium-quality spectroscopic performance by using NaI(Tl) and $CeBr_3$ scintillators, respectively. The mechanical collimator enables the detector to operate as a gamma camera, based on the original Anger Camera concept (Anger, 1964). An Anger camera utilizes a parallel-hole collimator to restrict γ rays entering the system and improves on the simple pinhole camera by utilizing a position-sensitive detecting system. This originally comprised a large scintillator detector and multiple photo-multiplier tubes. Such a detection setup enables the interaction point of an incidentγ ray within the detecting medium to be constrained, while the collimator allows γ rays of only certain incident angles to enter the system. This enables imaging at a range of distances but still severely reduces the number of γ rays that can enter the system, resulting in a low imaging efficiency. The efficiency can be increased by widening the collimator holes but again at the expense of image quality. In a pinhole and parallel-hole collimator, the number of γ rays reaching the detector may only be 0.01%–0.1% of those emitted by the source (Barrett, 1972). The collimator enables γ-ray imaging but with a restricted field of view (FoV), meaning that multiple angles must be imaged in a large decommissioning environment, such as a contaminated wall. To image high-energy γ rays above 400 keV with a collimated gamma camera, a thick collimator must be mounted, so the sensitivity to low-energy γ rays is reduced significantly. In order to improve the collimator transmission efficiency, the concept of coded aperture imaging (Dicke, 1968) was developed. This design increases the efficiency of Anger camera by utilizing a collimator mask of a patterned design. The pattern allows more γ rays to pass through to the detector by creating more open space in the mask. The pattern of the γ rays interacting with the detecting medium situated behind the mask can then be de-convolved back into an image of the γ-ray origins. The coded aperture results in a

higher imaging efficiency detector than a parallel-hole collimator, with typically 1% of emitted γ rays passing through the collimator to the detector behind (Meikle et al., 2001). However, this severely reduces the FoV that can be imaged to typically less than 50° (Woodring et al., 1999), and the range of energies is also limited. High-energy γ rays are difficult to stop (Phlips et al., 2002) and can penetrate the mask and result in interactions that are not related to the coded aperture. This reduces the image quality and prevents efficient imaging of γ rays above several hundred keV. Off-axis-originating γ rays can also interfere with the image and produce artifacts that must be removed. Generally, the mask must also be rotated and more data taken in order to prevent artifacts arising in the images. Further improvements in camera efficiency can be obtained by using an alternative methodology based on electronic collimation. Compton gamma cameras were first proposed for medical imaging applications in 1974 (Todd et al., 1974). Instead of a mechanical collimator in front of a position-sensitive detector, a second detector is generally used to exploit the kinematics of Compton scattering and so enable back projection of the γ-ray path. Compton imaging is performed by recording two (or more) γ interactions and, using Compton kinematics and Equation 1, back-projecting the possible γ paths based on their energy depositions.

$$\cos(\theta) = 1 + mc^2 \left(\frac{1}{E_1 + E_2} - \frac{1}{E_2} \right). \tag{1}$$

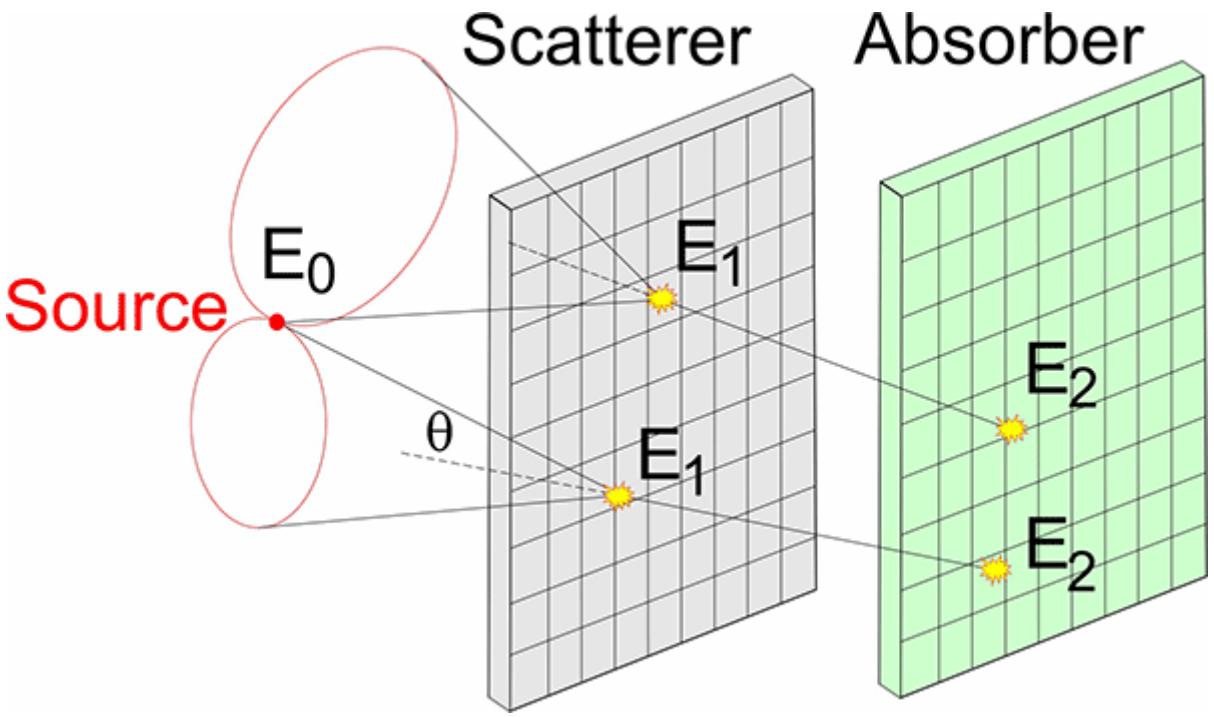

Figure 15. Diagram of a Compton camera system composed of two position-sensitive, planar Ge detectors. An incoming γ ray of energy E_0 Compton scatters in the front-layer depositing energy E_1 and is then photoelectrically absorbed in the second layer, depositing the rest of its energy, E_2. Cones, reconstructed with a knowledge the position and energy of each interaction is indicated for two events.

A diagram of a basic detector setup that can be used to perform Compton imaging is presented in Figure 15. This example comprises of two planar Ge detectors arranged in a series. The detectors are pixelated in order to provide position information of γ-ray interactions. An incoming γ ray from a source of energy E_0 undergoes Compton scattering, depositing energy, E_1, in the first detector before scattering forward toward the second detector, where it is absorbed, leaving the rest of its energy, E_2. Using Equation 1 with the knowledge of energy and position of both interactions, then the location of the source is calculated to be on the surface of a cone. Through the stacking of many of these events, two are shown in Figure 15, the area of highest conic overlap is the most likely origin of γ rays. In this manner, γ-ray imaging can be achieved with a two-layer Compton camera. A single detector can be used if the two interactions within it can be de-convolved into separate points. The more precisely the energy and position of the two interactions can be measured, the lower the uncertainty in the angle through which the cone has been back-projected, resulting in higher image quality. This device, compared with a collimated system, allows sensitivity to, and imaging of, a broad energy range in the region of 100 keV to 2 MeV over a wide FoV and with a high efficiency.

Compton camera imaging is possible with detectors with single pixelated crystals that have 3D-position capability. Transportable Compton camera–based solutions exist commercially. Two are a Ge γ-ray Imager (GeGi; Dryer et al., 2014), manufactured by PHDS, and a cadmium zinc telluride imager, Polaris-H (Wahl et al., 2015), manufactured by H3D. Such single-detector Compton imaging limits the image resolution possible due to the small separation between interactions within the detector. GeGi may also be operated with a pinhole collimator in order to provide high-precision images, but this lowers the system efficiency drastically. Likewise, Polaris-H is hampered by the medium-quality energy resolution of the Cadmium Zinc Telluride (CZT) crystal and the effect of Doppler broadening (Ordonez et al., 1997), so the image quality is degraded. This is due to the uncertainty introduced to the angles in Compton scattering as a result of uncertainty in the recorded incident γ-ray energy. Both systems provide 4π imaging capabilities for energy ranges of up to 1 MeV for GeGi (Dryer et al., 2014) and <2 MeV for Polaris-H (Wahl et al., 2015). GeGi reports a spatial resolution of ≈6°, while Polaris-H reports an angular resolution of ≈20° and an intrinsic imaging efficiency of ≈2% (Wahl et al., 2014). Both systems are capable of producing 2D images only and so lack a large amount of contextual information about the distribution of the source of radiation. Compton camera systems do have the ability to provide 3D information from the location of the highest intensity of the overlap of the cones, but this is limited to near-field imaging because here parallax effects in the detector system are significant. At larger distances, this can only be recovered by measuring the location of the source from more than one location and/or by fusing information from more than one imaging modality.

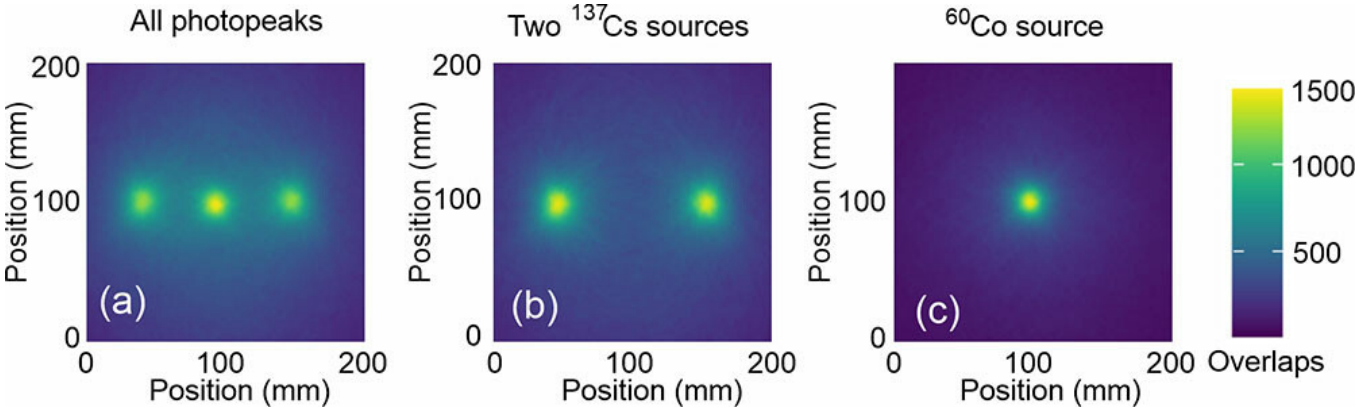

Figure 16. Compton slices of the intersecting cones produced from Compton camera analysis from the GRI+ spectrometer. The colored scale represents the numbers of overlaps of the Compton cones, see Figure 15. (a) Slices with all photopeaks selected. (b) ^{60}Co photopeaks selected. (c) ^{137}Cs photopeak selected.

Techniques are therefore being used to provide a more comprehensive image of the radiation sources and their environment. These approaches use the fusion of spectroscopic and imaging data with photographic and laser images of the location. This "scene-data fusion" provides a complete image of the environment in which the γ-ray sources are located and so can contextualize the γ image for the observer. Scene-data fusion is a technique used in γ-ray imaging for nuclear security, safety, and decommissioning purposes (Vetter, 2016; Vetter et al., 2018 and references therein). This type of scene-data fusion can be found in the Polaris-H (Wahl et al., 2015) and N-Visage systemsmanufactured by the company CREATEC (CREATEC, 2023), which both utilize integrated optical cameras in addition to γ imaging. These two systems also make use of point-cloud-generating laser systems, which are commonly found in mapping devices such as Light Detection And Ranging (LiDAR) systems and the Xbox Kinect, the latter of which is employed on the second generation Compact Compton Imager (Vetter, 2016) γ imaging system. LiDAR systems use pulsed lasers to measure the distances of objects. LiDAR systems are not affected by light levels and can provide very high sample densities, making them suitable for imaging in nuclear decommissioning environments where optical contrast, due to low light levels, is a common issue. An example of the capability of gamma-ray imaging and isotopic identification from a Compton camera and scene-data fusion is the GRI+ system (Caffrey et al., 2021). This transportable system is ideal for use for nuclear decommissioning and environmental and general radiation monitoring. It comprises a Compton camera with two double-sided strip detectors (one Si(Li) and one HPGe) and an extra HPGe coaxial detector for additional efficiency for high-energy gamma detection. Figure 16 shows Compton slice images from this system for three sources (two ^{137}Cs and one ^{60}Co) placed approximately 4 in. (10.5 cm) in front of the spectrometer. The position of the sources is clearly displayed and by selecting energy conditions on the photopeaks the type of source can be characterized. Figure 17 shows a LiDAR image of a typical complex industrial environment fused with a Compton camera image of a distributed ^{137}Cs source close to the concrete wall. The additional contextual information provided by the combination of the γ imaging data with the LIDAR 3D data allows for the true location of the

distributed source to be identified. These approaches are being utilized by the new generation of γ imagers under development. Research work is continuing to improve methodologies to provide quantification of the activity of the radioactive material identified in the FoV of these images.

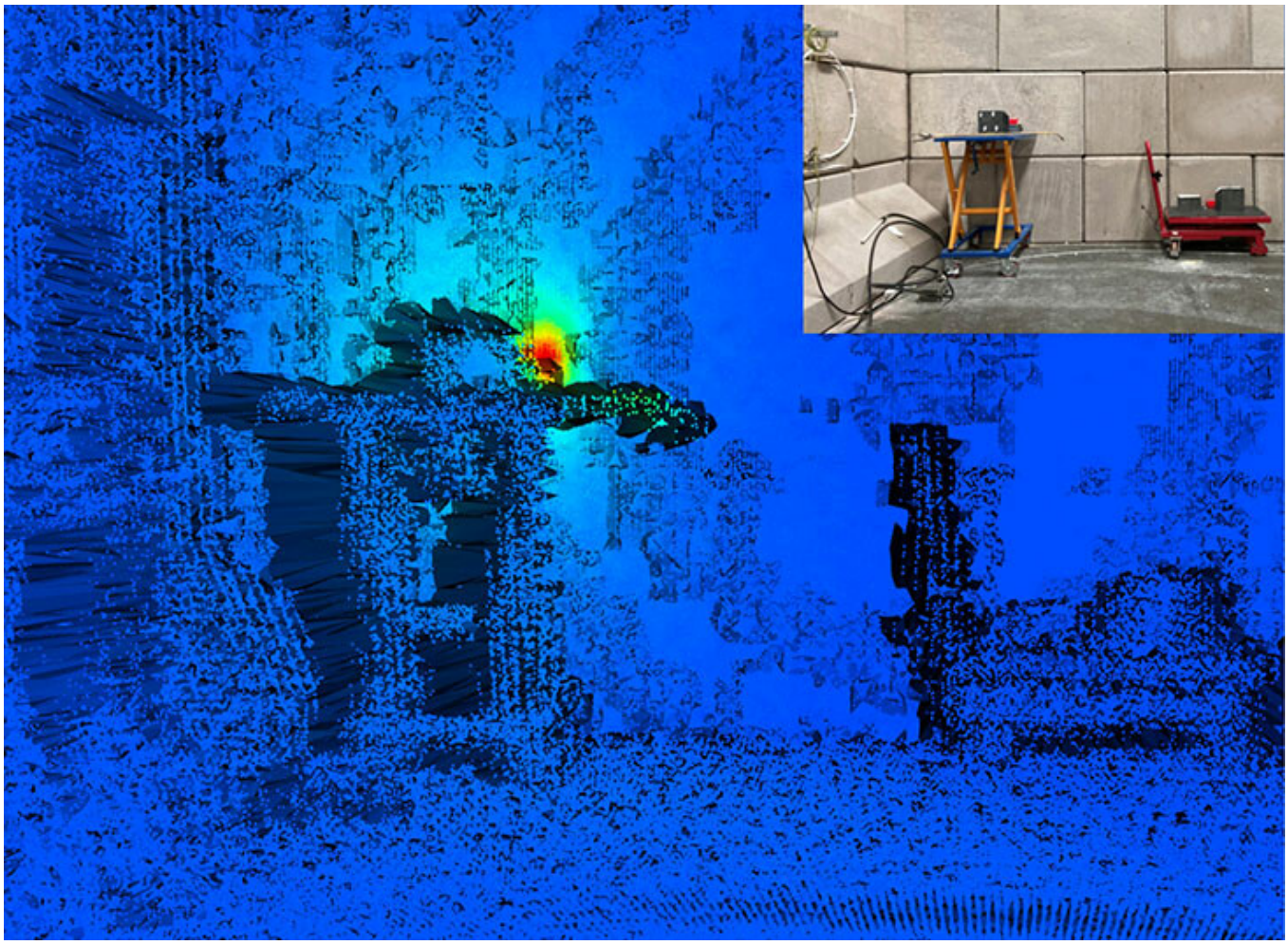

Figure 17. Light Detection And Ranging image (LiDAR) fused with Compton camera image obtained from the GRI+ system. A distributed ^{137}Cs source close to the concrete wall is visible behind partial lead shielding. A photograph of the environment is also shown.

4.1.1 Well and Point Contact Detectors

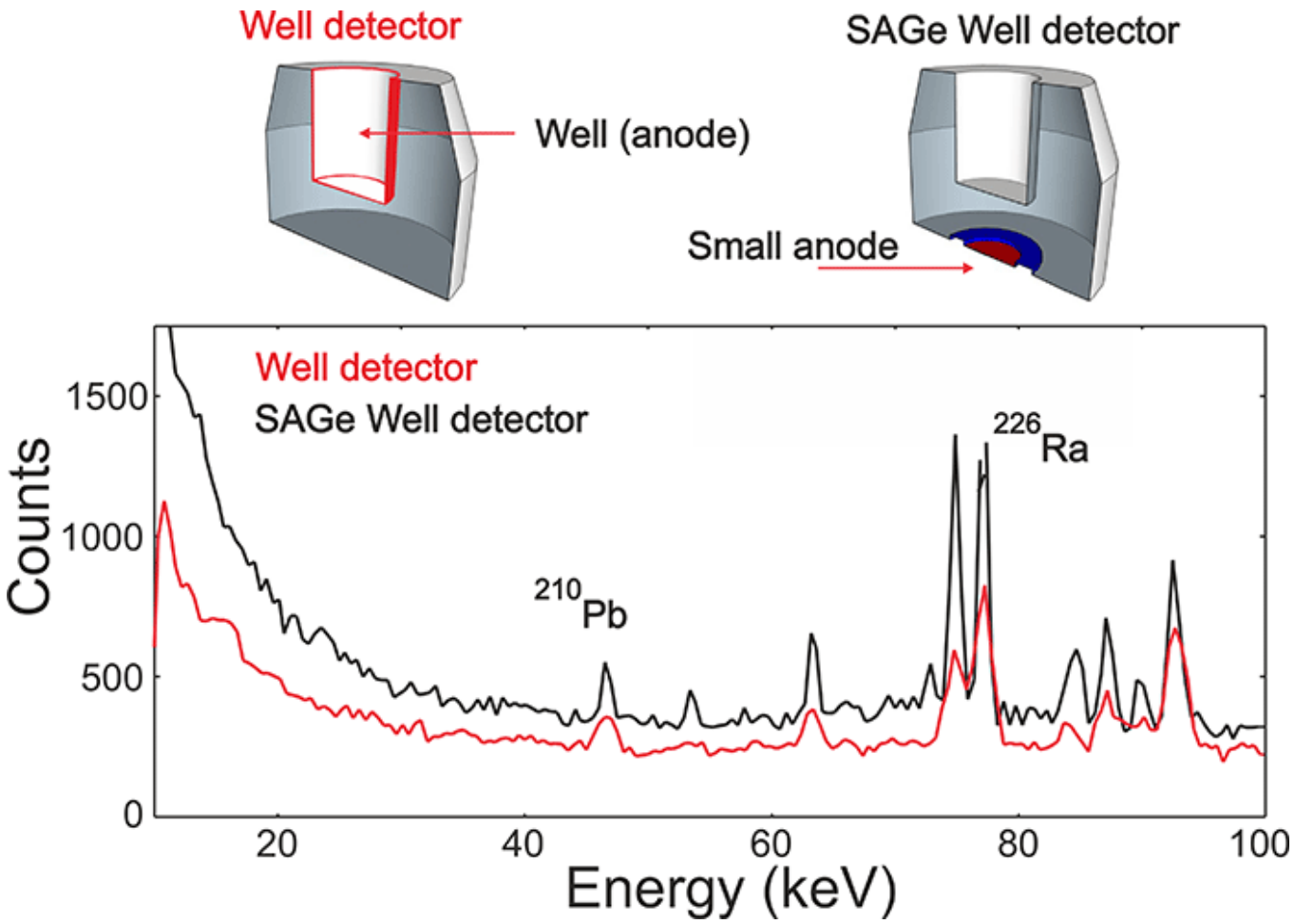

Figure 18. Spectra obtained with a conventional well detector and a small anode Ge (SAGe) well detector from a sediment lake sample. The images are simple schematic views of the Ge crystal. The improvement in resolution with the smaller charge collection anode is clearly displayed.

Ge detectors have excellent energy resolution and good efficiency and are the best for high-resolution γ-ray spectroscopy for nuclear science and applications. However, in some applications, there is a requirement for high efficiency but with even better resolution and as low a background as possible. A solution to this is the use of point contact HPGe detectors in an inverted coaxial geometry (Cooper et al., 2011; Luke et al., 1989). The small contact enables a much better energy resolution and an excellent signal-to-noise ratio to be achieved.

In applications such as environmental measurements, an excellent energy resolution and a high detection efficiency enable the identification of the origin of the naturally occurring and man-made isotopes in a sample and their specific activities. In cases in which sample sizes are limited, a well geometry, where the source is located inside the detector volume, is often used to maximize efficiency. One example of this application is for ^{210}Pb and ^{226}Ra measurements for direct gamma assay. These measurements can provide a record of changing concentrations in

lake sediments sufficiently reliable and precise to form a suitable basis for age/depth and dry sedimentation rate calculations (Appleby et al., 1986). Traditionally, Ge well detectors based on a p-type closed-end coaxial geometry have been used to collect the sample data. However, in the last decade, the Small Anode Ge Well detector (Adekola et al., 2015; Unsworth et al., 2019), manufactured by Mirion Technologies, has offered significant improvements in the energy resolution due to the reduced capacitance of the small contact when compared with the conventional coaxial well contact, see Figure 18. Indeed, the energy resolution for the 46 keV transition in ^{210}Pb is approximately a factor of 2 better.

A Ge point contact detector has been chosen for the 1-tonne scale LEGEND project (Abgrall et al., 2017), which is aimed at studying neutrino-less double-β decay to shed light on the fundamental properties of the neutrino, such as its mass and if it is a Majorana particle. The project will search for $0\nu\beta\beta$ decay in ^{76}Ge using isotopically enriched ^{76}Ge as the detector itself. These detectors were successfully tested in the GERmanium Detector Array (GERDA) (Agostini et al., 2017) and Majorana demonstrator projects (Aalseth et al., 2018). The characterization procedures, PSA, and tracking algorithms developed for GRETINA have been adapted for this new project.

Further developments of the inverted coaxial Ge detector are in progress with the production of highly segmented crystals. These developments include n-type (Salathe et al., 2017) and p-type (Pearce, 2020; Pearce et al., 2022; Wright et al., 2018) prototype detectors. The demonstrated performance of these detectors indicates not only an improvement in the energy resolution but perhaps, more importantly, an improvement in the achievable position resolution as well. In the future, these designs could be exploited in the next generation of γ spectrometers.

5. Summary and Outlook

This review has focused on the development of Ge detectors and arrays for scientific discoveries in nuclear physics research and in a variety of applications. The key technical advances have included the development of Ge(Li) and hyper-pure Ge detectors for high-resolution spectroscopy, the use of ESSs to improve the spectral signal-to-noise ratio, the use of arrays of detectors to increase the efficiency, and the realization of γ-ray tracking. At each stage, the level of sensitivity significantly improved to enable new phenomena in nuclear physics to be observed and understood. The latest development is γ-ray tracking and two projects, AGATA and GRETINA/GRETA, are being constructed to realize a complete 4π shell of highly segmented Ge detectors. The most important aspects of these projects, discussed in this work, are the detectors, the digital electronics and acquisition system, PSA, and tracking algorithms. These have been realized and successful scientific campaigns have already been performed in both projects. They have operated in several laboratories to take advantage of different beams (stable and radioactive), spectrometers, and complementary detectors. The science that these instruments will address covers a wide range of nuclear science at the extremes of excitation energy, spin, stability, and mass. The predicted sensitivity is expected to be two orders of magnitude better that the previous arrays of ESSs. The websites for these projects have the up-to-date status, plans, and scientific and technical publications (GRETA, 2023; Nyberg, 2023).

Although the technical advances made so far are impressive, further improvements are continually being implemented or planned.

The possibility of using digital cold preamplifiers is being considered for the detectors, which, in theory, would reduce noise and hence improve resolution.

PSA relies on there being a good understanding of the operational parameters of each detector in the array. Factors such as the crystal temperature, the unique charge-trapping profile in each crystal, and the electron–hole mobility values need further work to be properly understood. Closed-end coaxial detectors, such as the AGATA detectors, also suffer from divergence of the charge cloud as the holes approach the outer segmented contacts, which, for example, can result in the incorrect identification of a single interaction as a multiple interaction event. Again, improvement to the models used to describe the detector response function is required.

Improvement to the signal data basis continues to be a focus. The calculated basis requires improved knowledge of the key input parameters required for each detector, and factors such as the impurity gradients and knowledge of the passivated surface at the back of the crystal require more comprehensive information on the detector production or more detailed characterization measurements.

PSA and tracking algorithms are being optimized for a better position-of-interaction response, and an overall increase in data processing throughput in the system is desirable. The use of graphics processing units, high-performance computing facilities, machine learning, artificial intelligence, self-calibration of pulse shapes, and neural network approaches are being investigated.

Tracking technology is making possible the realization of a 3D spectroscopic “photograph” of a γ radiation field. This has wide applications in medical imaging, nuclear decommissioning, environmental monitoring, and security. There are countless examples of projects in each area, and just a few have been discussed. The use of a Compton camera incorporating the fusing of spectroscopic and stereoscopic imaging is presented. An example of environmental monitoring and nuclear dating using a small anode Ge “well” detector is given. Finally, the field of neutrino physics is also taking advantage of tracking technologies and detector innovations where an inverted closed-end Ge point contact detector is being used for the LEGEND project for neutrino-less double-beta-decay studies.

Additional reviews on the development of Ge detectors for nuclear spectroscopy can be found in, for example, Beausang and Simpson (1996), Eberth and Simpson (2008), Lee et al. (2003), Nolan et al. (1994), Riley et al. (2016), and Sharpey-Schafer and Simpson (1988).

Acknowledgments

This review is a result of the hard work and expertise of many people in many organizations. The authors would like to thank all those involved, especially those in the AGATA and GRETINA/GRETA projects. The authors are funded by grants from the U.K. Science and Technology Facilities Council, including ST/F004052/1, ST/T000554/1, and ST/V001027/1.

Data Access Statement: Data sharing is not applicable to this article as no data sets were generated or analyzed during this study.

References

Aalseth, C., Abgrall, N., Aguayo, E., Alvis, S. I., Amman, M., Arnquist, I. J., Avignone, F. T., Back, H. O., Barabash, A. S., Barbeau, P. S., Barton, C. J., Barton, P. J., Bertrand, F. E., Bode, T., Bos, B., Boswell, M., Bradley, A. W., Brodzinski, R. L., Brudanin, V., . . . Zimmermann, S. (2018). Search for Neutrinoless Double-β Decay in ^{76}Ge with the Majorana Demonstrator <https://doi.org/10.1103/physrevlett.120.132502>. *Physical Review Letters*, *120*, 132502.

Abgrall, N., Abramov, A., Abrosimov, N., Abt, I., Agostini, M., Agartioglu, M., Ajjaq, A., Alvis, S. I., Avignone, F. T., Bai, X., Balata, M., Barabanov, I., Barabash, A. S., Barton, P. J., Baudis, L., Bezrukov, L., Bode, T., Bolozdynya, A., Borowicz, D., . . . Zuzel, G. (2017). The large enriched germanium experiment for neutrinoless double beta decay (LEGEND) <https://doi.org/10.1063/1.5007652>. *AIP Conference Proceedings*, *1894*(1).

Adekola, A., Colaresi, J., Douwen, J., Mueller, W., & Yocum, K. (2015). Performance of a Small Anode Germanium Well detector <https://doi.org/10.1016/j.nima.2014.12.034>. *Nuclear Instruments and Methods in Physics Research Section A: Accelerators, Spectrometers, Detectors and Associated Equipment*, *784*(1), 124–130.

Agostinelli, S., Allison, J., Amako, K., Apostolakis, J., Araujo, H., Arce, P., Asai, M., Axen, D., Banerjee, S., Barrand, G., Behner, F., Bellagamba, L., Boudreau, J., Broglia, L., Brunengo, A., Burkhardt, H., Chauvie, S., Chuma, J., Chytracek, R., . . . Zschiesche, D. (2003). Geant4—a simulation toolkit <https://doi.org/10.1016/s0168-9002(03)01368-8>. *Nuclear Instruments and Methods in Physics Research Section A: Accelerators, Spectrometers, Detectors and Associated Equipment*, *506*(3), 250–303.

Agostini, M., Allardt, M., Bakalyarov, A. M., Balata, M., Barabanov, I., Baudis, L., Bauer, C., Bellotti, E., Belogurov, S., Belyaev, S. T., Benato, G., Bettini, A., Bezrukov, L., Bode, T., Borowicz, D., Brudanin, V., Brugnera, R., Caldwell, A., Cattadori, C., . . . Zuzel, G. (2017). Background-free search for neutrinoless double-β decay of ^{76}Ge with GERDA <https://doi.org/10.1038/nature21717>. *Nature*, *544*(7648), 47–52.

Akkoyun, S., Algora, A., Alikhani, B., Ameil, F., de Angelis, G., Arnold, L., Astier, A., Ataç, A., Aubert, Y., Aufranc, C., Austin, A., Aydin, S., Azaiez, F., Badoer, S., Balabanski, D., Barrientos, D., Baulieu, G., Baumann, R., Bazzacco, D., . . . Zucchiatti, A. (2012). AGATA—Advanced GAmma Tracking Array <https://doi.org/10.1016/j.nima.2011.11.081>. *Nuclear Instruments and Methods in Physics Research Section A: Accelerators, Spectrometers, Detectors and Associated Equipment*, *668*, 26–58.

Alexander, T., Broude, C., Häusser, O., & Sharpey-Schafer, J. (1968). A pair and escape-suppressed spectrometer using Ge(Li) and NaI(Tl) detectors designed for accelerator experiments <https://doi.org/10.1016/0029-554x(68)90558-2>. *Nuclear Instruments and Methods*, *65*(2), 169–172.

Allison, J., Amako, K., Apostolakis, J., Arce, P., Asai, M., Aso, T., Bagli, E., Bagulya, A., Banerjee, S., Barrand, G., Beck, B., Bogdanov, A., Brandt, D., Brown, J., Burkhardt, H., Canal, P., Cano-Ott, D., Chauvie, S., Cho, K., . . . Yoshida, H. (2016). Recent developments in GEANT4 <https://doi.org/10.1016/j.nima.2016.06.125>. *Nuclear Instruments and Methods in Physics Research Section A: Accelerators, Spectrometers, Detectors and Associated Equipment*, *835*, 186–225.

Alvarez, C. R. (1993). The GASP array <https://doi.org/10.1080/10506899308221154>. *Nuclear Physics News*, *3*(3), 10–13.

Anger, A. O. (1964). Scintillation camera with multichannel collimators. *Journal of Nuclear Medicine*, *5*(6), 515–531.

Appleby, P., Nolan, P., & Gifford, D. (1986). ^{210}Pb dating by low background gamma counting <https://doi.org/10.1007/BF00026640>. *Hydrobiologia*, *143*, 21–27.

Azaiez, F. (1999). EXOGAM: A γ-ray spectrometer for radioactive beams <https://doi.org/10.1016/s0375-9474(00)88588-7>. *Nuclear Physics A*, *654*(1), 1003c–1008c.

Barrett, H. H. (1972). Fresnel zone plate imaging in nuclear medicine. *Journal of Nuclear Medicine*, *13*(6), 382–385.

Bazzacco, D. (2004). The advanced gamma ray tracking array AGATA <https://doi.org/10.1016/j.nuclphysa.2004.09.148>. *Nuclear Physics A*, *746*, 248–254.

Beausang, C., Forbes, S., Fallon, P., Nolan, P., Twin, P., Mo, J., Lisle, J., Bentley, M., Simpson, J., Beck, F., Curien, D., deFrance, G., Duchêne, G., & Popescu, D. (1992).Measurements on prototype Ge and BGO detectors for the Eurogam array <https://doi.org/10.1016/0168-9002(92)90084-h>. *Nuclear Instruments and Methods in Physics Research Section A: Accelerators, Spectrometers, Detectors and Associated Equipment*, *313*(1–2), 37–49.

Beausang, C. W., & Simpson, J. (1996). Large arrays of escape suppressed spectrometers for nuclear structure experiments <https://doi.org/10.1088/0954-3899/22/5/003>. *Journal of Physics G: Nuclear and Particle Physics*, *22*(5), 527–558.

Beck, F. A. (1984, October). Properties of large BaF_2 crystals, applications as fast and efficient gamma-ray detectors in the 4π-γcrystal castle array. In D. Shapira (Ed.), *Proceedings of the international conference on instrumentation for heavy ion nuclear research held at Oak Ridge National Laboratory* (Vol. 7, pp. 129–145). Harwood Academic Publishers.

Beetz, R., Posthumus, W., Boer, F. D., Maarleveld, J., Schaaf, A. V. D., & Konijn, J. (1977). An in-beam Ge(Li)-NaI(Tl) Compton suppression spectrometer <https://doi.org/10.1016/0029-554x(77)90432-3>. *Nuclear Instruments and Methods*, *145*(2), 353–357.

Boso, A., Milne, S. A., Bentley, M., Recchia, F., Lenzi, S., Rudolph, D., Labiche, M., Pereira-Lopez, X., Afara, S., Ameil, F., Arici, T., Aydin, S., Axiotis, M., Barrientos, D., Benzoni, G., Birkenbach, B., Boston, A., Boston, H., Boutachkov, P., . . . Wieland, O. (2019). Isospin dependence of electromagnetic transition strengths among an isobaric triplet <https://doi.org/10.1016/j.physletb.2019.134835>. *Physics Letters B*, *797*, 134835.

Bracco, A. (2017). The NuPECC long range plan 2017: Perspectives in nuclear physics <https://doi.org/10.1080/10619127.2017.1352311>. *Nuclear Physics News*, *27*(3), 3–4.

Bracco, A., Duchêne, G., Podolyák, Z., & Reiter, P. (2021). Gamma spectroscopy with AGATA in its first phases: New insights in nuclear excitations along the nuclear chart <https://doi.org/10.1016/j.ppnp.2021.103887>. *Progress in Particle and Nuclear Physics*, *121*, 103887.

Bruyneel, B., Birkenbach, B., & Reiter, P. (2016). Pulse shape analysis and position determination in segmented HPGe detectors: The AGATA detector library <https://doi.org/10.1140/epja/i2016-16070-9>. *The European Physical Journal A*, *52*, Article 70.

Bruynell, B., Reiter, P., Weins, A., Eberth, J., Hess, H., Pascovici, G., Warr, N., Aydin, S., Bazzacco, D., & Recchia, F. (2009). Crosstalk corrections for improved energy resolution with highly segmented HPGe-detectors <https://doi.org/10.1016/j.nima.2009.06.037>. *Nuclear Instruments and Methods in Physics Research Section A: Accelerators, Spectrometers, Detectors and Associated Equipment*, *608*(1), 99–106.

Bruynell, B., Reiter, P., Wiens, A., Eberth, J., Hess, H., Pascovici, G., Warr, N., & Weisshaar, D. (2009). Crosstalk properties of 36-fold segmented symmetric hexagonal HPGe detectors <https://doi.org/10.1016/j.nima.2008.11.011>. *Nuclear Instruments and Methods in Physics Research Section A: Accelerators, Spectrometers, Detectors and Associated Equipment*, *599*(2–3), 196–208.

Burde, J., Dines, E. L., Shih, S., Diamond, R. M., Draper, J. E., Lindenberger, K. H., Schück, C., & Stephens, F. S. (1982). Third Discontinuity in the Yrast Levels of ^{158}Er <https://doi.org/10.1103/physrevlett.48.530>. *Physical Review Letters*, *48*(8), 530–533.

Caffrey, A., Harkness-Brennan, L., Alshammari, H., Boston, A., Boston, H., Griffiths, O., Judson, D., Kalantan, S., Crom, B. L., Nolan, P., Powell, A., Platt, J., Randall, G., Reid, C., Rintoul, E., Unsworth, C., Woodroof, T., Burrows, I., Lazarus, I., . . . Atkinson, K. (2021). Gamma-ray imaging performance of the GRI+ Compton camera <https://doi.org/10.1088/1748-0221/16/09/p09015>. *Journal of Instrumentation*, *16*(9), P09015.

Cavendish Nuclear. (2019). *RadScan 900* <https://www.cavendishnuclear.com/wp-content/uploads/2022/03/RadScan-900-Products-and-Services-2019_10.pdf>.

Cederwall, B., Liu, X., Aktas, Ö., Ertoprak, A., Zhang, W., Qi, C., Clément, E., de France, G., Ralet, D., Gadea, A., Goasduff, A., Jaworski, G., Kuti, I., Nyakó, B., Nyberg, J., Palacz, M., Wadsworth, R., Valiente-Dobón, J., Al-Azri, H., . . . Zielińska, M. (2020). Isospin Properties of Nuclear Pair Correlations from the Level Structure of the Self-Conjugate Nucleus ^{88}Ru <https://doi.org/10.1103/physrevlett.124.062501>. *Physical Review Letters*, *124*, 062501.

Clément, E., Michelagnoli, C., de France, G., Li, H., Lemasson, A., Dejean, C. B., Beuzard, M., Bougault, P., Cacitti, J., Foucher, J.-L., Fremont, G., Gangnant, P., Goupil, J., Houarner, C., Jean, M., Lefevre, A., Legeard, L., Legruel, F., Maugeais, C., . . . Rudigier, M. (2017). Conceptual design of the AGATA 1π array at GANIL <https://doi.org/10.1016/j.nima.2017.02.063>. *Nuclear Instruments and Methods in Physics Research Section A: Accelerators, Spectrometers, Detectors and Associated Equipment*, *855*, 1–12.

Collado, J., Capra, S., Pullia, A., Karkour, N., Houarner, C., Gonzalez, V., Wittwer, G., Boujrad, A., Kogimtzis, M., Lawson, J., Goasduff, A., Stezowski, O., Bonnin, C., Charles, L., Alaphilippe, V., Dosme, N., Esnault, C., Gibelin, L., Lafay, X., . . . Gadea, A. (2023). AGATA phase 2 advancements in front-end electronics <https://doi.org/10.1140/epja/s10050-023-01045-0>.*The European Physical Journal A*, *59*, 133.

Colosimo, S., Moon, S., Boston, A., Boston, H., Cresswell, J., Harkness-Brennan, L., Judson, D., Lazarus, I., Nolan, P., Simpson, J., & Unsworth, C. (2015). Characterisation of two AGATA asymmetric high purity germanium capsules <https://doi.org/10.1016/j.nima.2014.09.055>. *Nuclear Instruments and Methods in Physics Research Section A: Accelerators, Spectrometers, Detectors and Associated Equipment*, *773*, 124–136.

Cooper, R., Radford, D., Hausladen, P., & Lagergren, K. (2011). A novel HPGe detector for gamma-ray tracking and imaging <https://doi.org/10.1016/j.nima.2011.10.008>. *Nuclear Instruments and Methods in Physics Research Section A: Accelerators, Spectrometers, Detectors and Associated Equipment*, *665*, 25–32.

CREATEC. (2023). *N-Visage Gamma Imager* <https://www.createc.co.uk/case_study/blue-bear/>.

Crespi, F. C. L., Ljungvall, J., Lopez-Martens, A., & Michelagnoli, C. (2023). AGATA: performance of γ-ray tracking and associated algorithms <https://doi.org/10.1140/epja/s10050-023-01019-2>. *The European Physical Journal A*, *A59*, 111.

Deleplanque, M., Lee, I., Vetter, K., Schmid, G., Stephens, F., Clark, R., Diamond, R., Fallon, P., & Macchiavelli, A. (1999). GRETA: Utilizing new concepts in γ-ray detection <https://doi.org/10.1016/s0168-9002(99)00187-4>. *Nuclear Instruments and Methods in Physics Research Section A: Accelerators, Spectrometers, Detectors and Associated Equipment*, *430*(2–3), 292–310.

Descovich, M., Lee, I., Fallon, P., Cromaz, M., Macchiavelli, A., Radford, D., Vetter, K., Clark, R., Deleplanque, M., Stephens, F., & Ward, D. (2005). In-beam measurement of the position resolution of a highly segmented coaxial germanium detector <https://doi.org/10.1016/j.nima.2005.07.016>. *Nuclear Instruments and Methods in Physics Research Section A: Accelerators, Spectrometers, Detectors and Associated Equipment*, *553*(3), 535–542.

Diamond, R. M. (1985, October). The Berkeley high-resolution ball. In D. Shapira (Ed.), *Proceedings of the international conference on instrumentation for heavy ion nuclear research held at Oak Ridge National Laboratory* (Vol. 7, pp. 259–281). Harwood Academic Publishers.

Dicke, R. H. (1968). Scatter-Hole Cameras for X-Rays and Gamma Rays <https://doi.org/10.1086/180230>. *The Astrophysical Journal*, *153*, L101.

Dryer, J., Burks, M., & Hull, E. (2014, October). *Next Generation Germanium Systems for Safeguards Applications* <https://phdsco.com/wp-content/uploads/2020/04/2014_12_15_Paper.pdf>. Symposium on International Safeguards: Linking Strategy, Implementation and People - IAEA CN-220, Vienna, Austria.

Duchêne, G., Beck, F., Twin, P., de France, G., Curien, D., Han, L., Beausang, C., Bentley, M., Nolan, P., & Simpson, J. (1999). The Clover: a new generation of composite Ge detectors <https://doi.org/10.1016/s0168-9002(99)00277-6>. *Nuclear Instruments and Methods in Physics Research Section A: Accelerators, Spectrometers, Detectors and Associated Equipment*, *432*(1), 90–110.

Eberth, J. (1997). Development of segmented Ge detectors for future γ-ray arrays <https://doi.org/10.1016/s0146-6410(97)00003-3>. *Progress in Particle and Nuclear Physics*, *38*, 29–37.

Eberth, J., Pascovici, G., Thomas, H., Warr, N., Weisshaar, D., Habs, D., Reiter, P., Thirolf, P., Schwalm, D., Gund, C., Scheit, H., Lauer, M., Duppen, P. V., Franchoo, S., Huyse, M., Lieder, R., Gast, W., Gerl, J., & Lieb, K. (2001). MINIBALL A Ge detector array for radioactive ion beam facilities <https://doi.org/10.1016/s0146-6410(01)00145-4>. *Progress in Particle and Nuclear Physics*, *46*(1), 389–398.

Eberth, J., & Simpson, J. (2008). From Ge(Li) detectors to gamma-ray tracking arrays–50 years of gamma spectroscopy with germanium detectors <https://doi.org/10.1016/j.ppnp.2007.09.001>. *Progress in Particle and Nuclear Physics*, *60*(2), 283–337.

Eberth, J., Thomas, H., Brentano, P., Lieder, R., Jäger, H., Kämmerfing, H., Berst, M., Gutknecht, D., & Henck, R. (1996). Encapsulated Ge detectors: Development and first tests <https://doi.org/10.1016/0168-9002(95)00794-6>. *Nuclear Instruments and Methods in Physics Research Section A: Accelerators, Spectrometers, Detectors and Associated Equipment*, *369*(1), 135–140.

Eberth, J., von Brentano, P., Teichert, W., Mylaeus, T., Lieder, R., Gast, W., Hebbinghaus, G., Jäger, H., Maier, K., Grawe, H., Kluge, H., Schwalm, D., Gerl, J., Hübel, H., Henck, R., & Gutknecht, D. (1990). Development of composite Ge detectors for EUROBALL <https://doi.org/10.1016/0375-9474(90)91183-r>. *Nuclear Physics A*, *520*, c669–c676.

Eube, E., Eberth, J., Eberth, U., Eichner, H., & Zobel, V. (1975). A “five-in-one” Ge(Li) spectrometer as compton polarimeter <https://doi.org/10.1016/0029-554x(75)90159-7>. *Nuclear Instruments and Methods*, *130*(1), 73–77.

Ewan, G., & Tavendale, A. (1964). Application of high resolution lithium-drift germanium gamma-ray spectrometers to high energy gamma-rays <https://doi.org/10.1016/0029-554x(64)90072-2>. *Nuclear Instruments and Methods*, *26*, 183–186.

Farnea, E., Recchia, F., Bazzacco, D., Kröll, T., Podolyák, Z., Quintana, B., & Gadea, A. (2010). Conceptual design and Monte Carlo simulations of the AGATA array <https://doi.org/10.1016/j.nima.2010.04.043>. *Nuclear Instruments and Methods in Physics Research Section A: Accelerators, Spectrometers, Detectors and Associated Equipment*, *621*(1–3), 331–343.

Freck, D. V., & Wakefield, J. (1962). Gamma-Ray Spectrum obtained with a Lithium-drifted p–i–n Junction in Germanium <https://doi.org/10.1038/193669a0>. *Nature*, *193*(4816), 669.

Gade, A., & Gelbke, C. (2010). The NSCL laboratory and the FRIB facility <https://doi.org/10.4249/scholarpedia.9651>. *Scholarpedia*, *5*(1), 9651.

Gadea, A., Farnea, E., Valiente-Dobón, J., Million, B., Mengoni, D., Bazzacco, D., Recchia, F., Dewald, A., Pissulla, T., Rother, W., de Angelis, G., Austin, A., Aydin, S., Badoer, S., Bellato, M., Benzoni, G., Berti, L., Beunard, R., Birkenbach, B., . . . Zucchiatti, A. (2011). Conceptual design and infrastructure for the installation of the first AGATA sub-array at LNL <https://doi.org/10.1016/j.nima.2011.06.004>. *Nuclear Instruments and Methods in Physics Research Section A: Accelerators, Spectrometers, Detectors and Associated Equipment*, *654*(1), 88–96.

GRETA. (2023). *Gamma Ray Energy Tracking Array* <http://greta.lbl.gov/>.

Habs, D. (1997). Physics with Ge-Miniball-arrays <https://doi.org/10.1016/s0146-6410(97)00016-1>. *Progress in Particle and Nuclear Physics*, *38*, 111–126.

Hall, R. N., & Soltys, T. J. (1971). High purity germanium for detector fabrication <https://doi.org/10.1109/tns.1971.4325857>. *IEEE Transactions on Nuclear Science*, *18*(1), 160–165.

Hansen, W. (1971). High-purity germanium crystal growing <https://doi.org/10.1016/0029-554x(71)90593-3>. *Nuclear Instruments and Methods*, *94*(2), 377–380.

Herskind, B. (1986). The NORDBALL — A multidetector system for the study of nuclear structure <https://doi.org/10.1016/0375-9474(86)90619-6>. *Nuclear Physics A*, *447*, 395–412.

Jääskeläinen, M., Sarantites, D., Woodward, R., Dilmanian, F., Hood, J., Jääskeläinen, R., Hensley, D., Halbert, M., & Barker, J. (1983). The spin spectrometer: Design, instrumentation and response characteristics of 4πγ-ray

multidetector system <https://doi.org/10.1016/0167-5087(83)90068-6>. *Nuclear Instruments and Methods in Physics Research*, *204*(2–3), 385–405.

John, P. R., Modamio, V., Valiente-Dobón, J. J., Mengoni, D., Lunardi, S., Rodrıguez, T. R., Bazzacco, D., Gadea, A., Wheldon, C., Alexander, T., de Angelis, G., Ashwood, N., Barr, M., Benzoni, G., Birkenbach, B., Bizzeti, P. G., Bizzeti-Sona, A. M., Bottoni, S., Bowry, M., . . . Walshe, J. (2014). Shape evolution in the neutron-rich osmium isotopes: Prompt γ-ray spectroscopy of ^{196}Os <https://doi.org/10.1103/physrevc.90.021301>. *Physical Review C*, *90*, 021301(R).

Johnson, A., Ryde, H., & Sztarkier, J. (1971). Evidence for a “singularity” in the nuclear rotational band structure <https://doi.org/10.1016/0370-2693(71)90150-x>. *Physics Letters B*, *34*(7), 605–608.

Khoo, T. L., Smither, R. K., Haas, B., Häusser, O., Andrews, H. R., Horn, D., & Ward, D. (1978). Yrast traps and very high-spin yrast states in ^{152}Dy <https://doi.org/10.1103/physrevlett.41.1027>. *Physical Review Letters*, *41*(15), 1027–1030.

Korichi, A., & Lauritsen, T. (2019). Tracking γ rays in highly segmented HPGe detectors: A review of AGATA and GRETINA <https://doi.org/10.1140/epja/i2019-12787-1>. *The European Physical Journal A*, *55*, 121.

Korten, W., Atac, A., Beaumel, D., Bednarczyk, P., Bentley, M. A., Benzoni, G., Boston, A., Bracco, A., Cederkäll, J., Cederwall, B., Ciemała, M., Clément, E., Crespi, F. C. L., Curien, D., de Angelis, G., Didierjean, F., Doherty, D. T., Dombradi, Z., Duchêne, G., . . . Zielińska, M. (2020). Physics opportunities with the Advanced Gamma Tracking Array: AGATA <https://doi.org/10.1140/epja/s10050-020-00132-w>. *The European Physical Journal A*, *56*, 137.

Kröll, T., & Bazzacco, D. (2001). Simulation and analysis of pulse shapes from highly segmented HPGe detectors for the γ-ray tracking array MARS <https://doi.org/10.1016/s0168-9002(01)00208-x>. *Nuclear Instruments and Methods in Physics Research Section A: Accelerators, Spectrometers, Detectors and Associated Equipment*, *463*(1–2), 227–249.

Labiche, M., Ljungvall, J., Crespi, F. C. L., Chen, S., Bordes, J., Goasduff, A., Bottoni, S., Gamba, E., Pérez-Vidal, R. M., & Bentley, M. A. (2023). Simulation of the AGATA spectrometer and coupling with ancillary detectors <https://doi.org/10.1140/epja/s10050-023-01036-1>. *The European Physical Journal A*, *59*, 158.

Lauritsen, T., Korichi, A., Zhu, S., Wilson, A., Weisshaar, D., Dudouet, J., Ayangeakaa, A., Carpenter, M., Campbell, C., Clément, E., Crawford, H., Cromaz, M., Fallon, P., Greene, J., Janssens, R., Khoo, T., Lalović, N., Lee, I., Macchiavelli, A., . . . Stezowski, O. (2016). Characterization of a gamma-ray tracking array: A comparison of GRETINA and Gammasphere using a 60Co source <https://doi.org/10.1016/j.nima.2016.07.027>. *Nuclear Instruments and Methods in Physics Research Section A: Accelerators, Spectrometers, Detectors and Associated Equipment*, *836*, 46–56.

Lee, I.-Y. (1990). The GAMMASPHERE <https://doi.org/10.1016/0375-9474(90)91181-p>. *Nuclear Physics A*, *520*, c641–c655.

Lee, I.-Y., Clark, R., Cromaz, M., Deleplanque, M., Descovich, M., Diamond, R., Fallon, P., Macchiavelli, A., Stephens, F., & Ward, D. (2004). GRETINA: A gamma ray energy tracking array <https://doi.org/10.1016/j.nuclphysa.2004.09.038>. *Nuclear Physics A*, *746*, 255–259.

Lee, I.-Y., Deleplanque, M. A., & Vetter, K. (2003). Developments in large gamma-ray detector arrays <https://doi.org/10.1088/0034-4885/66/7/201>. *Reports on Progress in Physics*, *66*(7), 1095–1144.

Lee, I.-Y., & Simpson, J. (2010). AGATA and GRETA: The Future of Gamma-Ray Spectroscopy <https://doi.org/10.1080/10619127.2010.506124>. *Nuclear Physics News*, *20*(4), 23–28.

Lieder, R., Jäger, H., Neskakis, A., Venkova, T., & Michel, C. (1984). Design of a bismuth germanate anti-Compton spectrometer and its use in nuclear spectroscopy <https://doi.org/10.1016/0167-5087(84)90297-7>. *Nuclear Instruments and Methods in Physics Research*, *220*(2–3), 363–370.

Lopez-Martens, A., Hauschild, K., Korichi, A., Roccaz, J., & Thibaud, J.-P. (2004). γ-ray tracking algorithms: a comparison <https://doi.org/10.1016/j.nima.2004.06.154>. *Nuclear Instruments and Methods in Physics Research Section A: Accelerators, Spectrometers, Detectors and Associated Equipment*, *533*(3), 454–466.

Luke, P., Goulding, F., Madden, N., & Pehl, R. (1989). Low capacitance large volume shaped-field germanium detector <https://doi.org/10.1109/23.34577>. *IEEE Transactions on Nuclear Science*, *36*(1), 926–930.

Martin, J., Radford, D., Beaulieu, M., Taras, P., Ward, D., Andrews, H., Ayotte, G., Sharp, F., Waddington, J., Häusser, O., & Gascon, J. (1987). Data acquisition system for the 8π spectrometer: A multidetector array for γ-ray spectroscopy <https://doi.org/10.1016/0168-9002(87)90749-2>. *Nuclear Instruments and Methods in Physics Research Section A: Accelerators, Spectrometers, Detectors and Associated Equipment*, *257*(2), 301–308.

Meikle, S., Fulton, R., Eberl, S., Dahlbom, M., Wong, K.-P., & Fulham, M. (2001). An investigation of coded aperture imaging for small animal SPECT <https://doi.org/10.1109/23.940169>. *IEEE Transactions on Nuclear Science*, *48*(3), 816–821.

Morinaga, H., & Gugelot, P. (1963). Gamma rays following (α, xn) reactions <https://doi.org/10.1016/0029-5582(63)90581-9>. *Nuclear Physics*, *46*, 210–224.

Nelson, L., Dimmock, M., Boston, A., Boston, H., Cresswell, J., Nolan, P., Lazarus, I., Simpson, J., Medina, P., Santos, C., & Parisel, C. (2007). Characterisation of an AGATA symmetric prototype detector <https://doi.org/10.1016/j.nima.2006.11.042>. *Nuclear Instruments and Methods in Physics Research Section A: Accelerators, Spectrometers, Detectors and Associated Equipment*, *573*(1–2), 153–156.

Nolan, P., Gifford, D., & Twin, P. (1985). The performance of a bismuth germanate escape suppressed spectrometer <https://doi.org/10.1016/0168-9002(85)90131-7>. *Nuclear Instruments and Methods in Physics Research Section A: Accelerators, Spectrometers, Detectors and Associated Equipment*, *236*(1), 95–99.

Nolan, P. J., Beck, F. A., & Fossan, D. B. (1994). Large arrays of escape-suppressed gamma-ray detectors <https://doi.org/10.1146/annurev.ns.44.120194.003021>. *Annual Review of Nuclear and Particle Science*, *44*(1), 561–607.

Nyberg, J. (2023). *AGATA* <https://www.agata.org/>.

Ordonez, C., Bolozdynya, A., & Chang, W. (1997, November). *Doppler broadening of energy spectra in Compton cameras* <https://doi.org/10.1109/nssmic.1997.670574>. 1997 IEEE Nuclear Science Symposium Conference Record, Albuquerque, NM, USA, 1361–1365.

Paschalis, S., Lee, I., Macchiavelli, A., Campbell, C., Cromaz, M., Gros, S., Pavan, J., Qian, J., Clark, R., Crawford, H., Doering, D., Fallon, P., Lionberger, C., Loew, T., Petri, M., Stezelberger, T., Zimmermann, S., Radford, D., Lagergren, K., . . . Beausang, C. (2013). The performance of the Gamma-Ray Energy Tracking In-beam Nuclear Array GRETINA <https://doi.org/10.1016/j.nima.2013.01.009>. *Nuclear Instruments and Methods in Physics Research Section A: Accelerators, Spectrometers, Detectors and Associated Equipment*, *709*, 44–55.

Paul, E. S., Twin, P. J., Evans, A. O., Pipidis, A., Riley, M. A., Simpson, J., Appelbe, D. E., Campbell, D. B., Choy, P. T. W., Clark, R. M., Cromaz, M., Fallon, P., Görgen, A., Joss, D. T., Lee, I. Y., Macchiavelli, A. O., Nolan, P. J., Ward, D., & Ragnarsson, I. (2007). Return of Collective Rotation in ^{157}Er and ^{158}Er at Ultrahigh Spin <https://doi.org/10.1103/physrevlett.98.012501>. *Physical Review Letters*, *98*, 012501.

Pearce, F. (2020). *Characterisation of the first p-type Segmented Inverted-coaxial Germanium Detector, SIGMA* <https://livrepository.liverpool.ac.uk/3124117/>. [PhD thesis, University of Liverpool].

Pearce, F., Harkness-Brennan, L., Alharbi, A., Boston, A., Griffiths, O., Holloway, F., Judson, D., Labiche, M., Nolan, P., Page, R., Radford, D., Rintoul, E., Simpson, J., Unsworth, C., & Wright, J. (2022). First experimental measurements with the Segmented Inverted-coaxial GerMAnium (SIGMA) detector <https://doi.org/10.1016/j.nima.2021.166044>. *Nuclear Instruments and Methods in Physics Research Section A: Accelerators, Spectrometers, Detectors and Associated Equipment*, *1027*, 166044.

Pell, E. M. (1960). Ion Drift in an n-p Junction <https://doi.org/10.1063/1.1735561>. *Journal of Applied Physics*, *31*(2), 291–302.

Phlips, B., Johnson, W., Kroeger, R., Kurfess, J., Phillips, G., Wulf, E., & Luke, P. (2002). Development of germanium strip detectors for environmental remediation <https://doi.org/10.1109/tns.2002.1003681>. *IEEE Transactions on Nuclear Science*, *49*(2), 597–600.

Pietralla, N., Reese, M., Cortes, M., Ameil, F., Bazzacco, D., Bentley, M., Boutachkov, P., Domingo-Pardo, C., Gadea, A., Gerl, J., Goel, N., Golubev, P., Górska, M., Guastalla, G., Habermann, T., Kojouharov, I., Korten, W., Merchán, E., Pietri, S., . . . Wollersheim, H. (2014). On the Road to FAIR: 1st Operation of AGATA in PreSPEC at GSI <https://doi.org/10.1051/epjconf/20146602083>. *European Physical Journal Web of Conferences*, *66*, 02083.

Recchia, F., Bazzacco, D., Farnea, E., Gadea, A., Venturelli, R., Beck, T., Bednarczyk, P., Buerger, A., Dewald, A., Dimmock, M., Duchene, G., Eberth, E., Faul, T., Gerl, G., Gernhaeuser, R., Hauschild, K., Holler, A., Jones, P., Korten, W., . . . Wesshaar, D. (2009). Position resolution of the prototype AGATA triple-cluster detector from an in-beam experiment <http://doi.org/10.1016/j.nima.2009.02.042>. *Nuclear Instruments and Methods in Physics Research Section A: Accelerators, Spectrometers, Detectors and Associated Equipment*, *604*(3), 555–562.

Riedinger, L. L., Andersen, O., Frauendorf, S., Garrett, J. D., Gaardhøje, J. J., Hagemann, G. B., Herskind, B., Makovetzky, Y. V., Waddington, J. C., Guttormsen, M., & TjØm, P. O. (1980). Frequency and alignment classification of multiple band crossings <https://doi.org/10.1103/physrevlett.44.568>. *Physical Review Letters*, *44*(9), 568–572.

Riley, M. A., Simpson, J., & Paul, E. S. (2016). High resolution gamma-ray spectroscopy and the fascinating angular momentum realm of the atomic nucleus <https://doi.org/10.1088/0031-8949/91/12/123002>. *Physica Scripta*, *91*, 123002.

Salathe, M., Cooper, R., Crawford, H., Radford, D., Allmond, J., Campbell, C., Clark, R., Cromaz, M., Fallon, P., Hausladen, P., Jones, M., Macchiavelli, A., & Wright, J. (2017). Energy reconstruction of an n-type segmented inverted coaxial point-contact HPGe detector <https://doi.org/10.1016/j.nima.2017.06.036>. *Nuclear Instruments and Methods in Physics Research Section A: Accelerators, Spectrometers, Detectors and Associated Equipment*, *868*, 19–26.

Schmid, G., Deleplanque, M., Lee, I., Stephens, F., Vetter, K., Clark, R., Diamond, R., Fallon, P., Macchiavelli, A., & MacLeod, R. (1999). A γ-ray tracking algorithm for the GRETA spectrometer <https://doi.org/10.1016/

s0168-9002(99)00188-6>. *Nuclear Instruments and Methods in Physics Research Section A: Accelerators, Spectrometers, Detectors and Associated Equipment*, *430*(1), 69–83.

Scraggs, H., Pearson, C., Hackman, G., Smith, M., Austin, R., Ball, G., Boston, A., Bricault, P., Chakrawarthy, R., Churchman, R., Cowan, N., Cronkhite, G., Cunningham, E., Drake, T., Finlay, P., Garrett, P., Grinyer, G., Hyland, B., Jones, B., . . . Zimmerman, L. (2005). TIGRESS highly-segmented high-purity germanium clover detector <https://doi.org/10.1016/j.nima.2004.12.012>. *Nuclear Instruments and Methods in Physics Research Section A: Accelerators, Spectrometers, Detectors and Associated Equipment*, *543*(2–3), 431–440.

Sharpey-Schafer, J., & Simpson, J. (1988). Escape suppressed spectrometer arrays: A revolution in γ-ray spectroscopy <https://doi.org/10.1016/0146-6410(88)90035-x>. *Progress in Particle and Nuclear Physics*, *21*, 293–400.

Shepherd, S., Nolan, P., Cullen, D., Appelbe, D., Simpson, J., Gerl, J., Kaspar, M., Kleinboehl, A., Peter, I., Rejmund, M., Schaffner, H., Schlegel, C., & de France, G. (1999). Measurements on a prototype segmented Clover detector <https://doi.org/10.1016/s0168-9002(99)00524-0>. *Nuclear Instruments and Methods in Physics Research Section A: Accelerators, Spectrometers, Detectors and Associated Equipment*, *434*(2–3), 373–386.

Simon, R. S. (1980). The Darmstadt-Heidelberg Crystal ball <https://doi.org/10.1051/jphyscol:19801031>. *Journal de Physique*, *41*, C10.

Simpson, J. (1997). The Euroball spectrometer <https://doi.org/10.1007/s002180050290>. *Zeitschrift für Physik A Hadrons and Nuclei*, *358*(2), 139–143.

Simpson, J., Azaiez, F., de France, G., Fouan, J., Gerl, J., Julin, R., Korten, W., Nyako, B., Sletten, G., & Walker, P. (2000). The EXOGAM Array: A radioactive Beam Gamma-Ray Spectrometer. *Acta Physica Hungarica, Series A: Heavy Ion Physics*, *11*, 159–188.

Simpson, J., Butler, P., & Ekström, L. (1983). Application of a sectored Ge(Li) detector as a Compton polarimeter <https://doi.org/10.1016/0167-5087(83)90074-1>. *Nuclear Instruments and Methods in Physics Research*, *204*(2–3), 463–469.

Simpson, J., Riley, M. A., Pipidis, A., Paul, E. S., Wang, X., Nolan, P. J., Sharpey-Schafer, J. F., Aguilar, A., Appelbe, D. E., Ayangeakaa, A. D., Boston, A. J., Boston, H. C., Campbell, D. B., Carpenter, M. P., Chiara, C. J., Choy, P. T. W., Clark, R. M., Cromaz, M., Evans, A. O., . . . Ragnarsson, I. (2023). Evolution of structure and shapes in ^{158}Er to ultrahigh spin <https://doi.org/10.1103/physrevc.107.054305>. *Physical Review C*, *107*, 054305.

Smith, R., Menegazzo, R., Aufranc, C., Bez, N., Burrows, I., Cahoreau, M., Debras, G., Gibelin, L., Goasduff, A., Grant, A., Joannem, T., Karkour, N., Karolak, M., Kieffer, J., Lotodé, A., Million, B., Morrall, P. S., Ramina, L., Rampazzo, M., . . . Zielińska, M. (2023). AGATA: Mechanics and infrastructures <https://doi.org/10.1140/epja/s10050-023-01046-z>. *The European Physical Journal A*, *59*, 166.

Stézowski, O., Dudouet, J., Goasduff, A., Korichi, A., Aubert, Y., Balogh, M., Baulieu, G., Bazzacco, D., Brambilla, S., Brugnara, D., Dosme, N., Elloumi, S., Gauron, P., Grave, X., Jacob, J., Lafage, V., Lemasson, A., Legay, E., Jeannic, P. L., . . . Toniolo, N. (2023). Advancements in software developments <https://doi.org/10.1140/epja/s10050-023-01025-4>. *The European Physical Journal A*, *59*, 119.

Tavendale, A., & Ewan, G. (1963). A high resolution lithium-drift germanium gamma-ray spectrometer <https://doi.org/10.1016/0029-554x(63)90183-6>. *Nuclear Instruments and Methods*, *25*, 185–187.

Todd, R. W., Nightingale, J. M., & Everett, D. B. (1974). A proposed γ camera <https://doi.org/10.1038/251132a0>. *Nature*, *251*(5471), 132–134.

Twin, P., Nolan, P., Aryaeinejad, R., Love, D., Nelson, A., & Kirwan, A. (1983). TESSA : A multi-detector γ-ray array designed to study high spin states <https://doi.org/10.1016/0375-9474(83)90696-6>. *Nuclear Physics A*, *409*, 343–351.

Twin, P. J. (1985). TESSA: Its present status and future development. In D. Shapira (Ed.), *Proceedings of the international conference on instrumentation for heavy ion nuclear research held at Oak Ridge National Laboratory, October 1984* (Vol. 7, pp. 231–257). Harwood Academic Publishers.

Twin, P. J., Nyakó, B. M., Nelson, A. H., Simpson, J., Bentley, M. A., Cranmer-Gordon, H. W., Forsyth, P. D., Howe, D., Mokhtar, A. R., Morrison, J. D., Sharpey-Schafer, J. F., & Sletten, G. (1986). Observation of a discrete-line superdeformed band up to 60ℏ in 152Dy <https://doi.org/10.1103/physrevlett.57.811>. *Physical Review Letters*, *57*(7), 811–814.

Unsworth, C., Boston, A., Boston, H., Harkness-Brennan, L., Judson, D., Nolan, P., Thomas, O., Wright, J., Adekola, A., Colaresi, J., Mueller, W., & Simpson, J. (2019). Characterisation of a small electrode HPGe detector <https://doi.org/10.1016/j.nima.2019.02.043>. *Nuclear Instruments and Methods in Physics Research Section A: Accelerators, Spectrometers, Detectors and Associated Equipment*, *927*, 293–300.

Valiente-Dobón, J., Pearson, C., Regan, P., Sellin, P., Gelletly, W., Morton, E., Boston, A., Descovich, M., Nolan, P., Simpson, J., Lazarus, I., & Warner, D. (2003). Performance of a 6×6 segmented germanium detector for γ-ray tracking <https://doi.org/10.1016/s0168-9002(03)01045-3>. *Nuclear Instruments and Methods in Physics Research Section A: Accelerators, Spectrometers, Detectors and Associated Equipment*, *505*(1–2), 174–177.

Venturelli, R., & Bazzacco, D. (2005). Adaptive grid search as pulse shape analysis algorithm for γ-tracking and results <https://www1.lnl.infn.it/%7Eannrep/read_ar/2004/index_2004.html>. [Legnaro National Laboratory, Annual Report 2004, pp. 220].

Vetter, K. (2016). Multi-sensor radiation detection, imaging, and fusion <https://doi.org/10.1016/j.nima.2015.08.078>. *Nuclear Instruments and Methods in Physics Research Section A: Accelerators, Spectrometers, Detectors and Associated Equipment*, *805*(1), 127–135.

Vetter, K., Barnowksi, R., Haefner, A., Joshi, T. H., Pavlovsky, R., & Quiter, B. J. (2018). Gamma-Ray imaging for nuclear security and safety: Towards 3-D gamma-ray vision <https://doi.org/10.1016/j.nima.2017.08.040>. *Nuclear Instruments and Methods in Physics Research Section A: Accelerators, Spectrometers, Detectors and Associated Equipment*, *878*, 159–168.

Vetter, K., Kuhn, A., Deleplanque, M., Lee, I., Stephens, F., Schmid, G., Beckedahl, D., Blair, J., Clark, R., Cromaz, M., Diamond, R., Fallon, P., Lane, G., Kammeraad, J., Macchiavelli, A., & Svensson, C. (2000). Three-dimensional position sensitivity in two-dimensionally segmented HP-Ge detectors <https://doi.org/10.1016/s0168-9002(00)00430-7>. *Nuclear Instruments and Methods in Physics Research Section A: Accelerators, Spectrometers, Detectors and Associated Equipment*, *452*(1–2), 223–238.

Wahl, C. G., Kaye, W., Wang, W., Zhang, F., Jaworski, J., Boucher, Y. A., King, A., & He, Z. (2014, November 14). Polaris-H measurements and performance <https://doi.org/10.1109/nssmic.2014.7431109>. In *2014 IEEE Nuclear Science Symposium and Medical Imaging Conference (NSS/MIC)* (pp. 1–4).

Wahl, C. G., Kaye, W. R., Wang, W., Zhang, F., Jaworski, J. M., King, A., Boucher, Y. A., & He, Z. (2015). The Polaris-H imaging spectrometer <https://doi.org/10.1016/j.nima.2014.12.110>. *Nuclear Instruments and Methods in Physics Research Section A: Accelerators, Spectrometers, Detectors and Associated Equipment*, *784*, 377–381.

Weisshaar, D., Bazin, D., Bender, P., Campbell, C., Recchia, F., Bader, V., Baugher, T., Belarge, J., Carpenter, M., Crawford, H., Cromaz, M., Elman, B., Fallon, P., Forney, A., Gade, A., Harker, J., Kobayashi, N., Langer, C., Lauritsen, T., . . . Zhu, S. (2017). The performance of the γ-ray tracking array GRETINA for γ-ray spectroscopy with fast beams of rare isotopes <https://doi.org/10.1016/j.nima.2016.12.001>. *Nuclear Instruments and Methods in Physics Research Section A: Accelerators, Spectrometers, Detectors and Associated Equipment*, *847*, 187–198.

Woodring, M., Souza, D., & Tipnis, S. (1999). Advanced radiation imaging of low-intensity gamma-ray sources <https://doi.org/10.1016/S0168-9002(98)01022-5>. *Nuclear Instruments and Methods in Physics Research Section A: Accelerators, Spectrometers, Detectors and Associated Equipment*, *422*, 709–712.

Wright, J., Harkness-Brennan, L., Boston, A., Judson, D., Labiche, M., Nolan, P., Page, R., Pearce, F., Radford, D., Simpson, J., & Unsworth, C. (2018). Position resolution simulations for the inverted-coaxial germanium detector, SIGMA <https://doi.org/10.1016/j.nima.2018.02.106>. *Nuclear Instruments and Methods in Physics Research Section A: Accelerators, Spectrometers, Detectors and Associated Equipment*, *892*, 84–92.

Wyss, R., & Riley, M. A. (2022). Fifty years of backbending <https://doi.org/10.1080/10619127.2022.2063000>. *Nuclear Physics News*, *32*(2), 16–20.